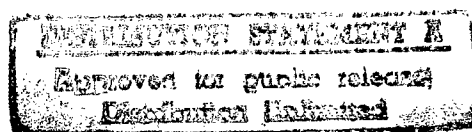




# ***JPRS Report***



# **Science & Technology**

## ***USSR: Materials Science***

19980113 382

**DTIC QUALITY INSPECTED 3**

REPRODUCED BY  
U.S. DEPARTMENT OF COMMERCE  
NATIONAL TECHNICAL INFORMATION SERVICE  
SPRINGFIELD, VA. 22161

# Science & Technology

## USSR: Materials Science

JPRS-UMS-91-007

### CONTENTS

19 July 1991

#### FERROUS METALS

Reduction of Deformation of Cylindrical Parts During Nitriding [I.S. Dukarevich; <i>METALLOVEDENIYE I TERMICHESKAYA OBRABOTKA METALLOV</i> , Dec 90]	1
Effect of Heat-Treatment Practice on Brittle-Fracture Resistance of Heavy-Plate Low-Alloy Steel 09G2S [V.M. Gornitskiy, G.R. Shneyderov, and T.G. Zaytseva; <i>METALLOVEDENIYE I TERMICHESKAYA OBRABOTKA METALLOV</i> , Dec 90]	1
Use of Water Solution of Technical Lignosulfonate for Quenching Heavy Steel Articles [V.Ye. Loshkarev, L.I. Sorokina, and S.A. Peskischev; <i>METALLOVEDENIYE I TERMICHESKAYA OBRABOTKA METALLOV</i> , Dec 90]	1
Ion Nitriding of Steel Kh12F1 [A.I. Slosman and N.M. Lemeshev; <i>METALLOVEDENIYE I TERMICHESKAYA OBRABOTKA METALLOV</i> , Dec 90]	1
Influence of Calcium and Barium Modification on Microstructure of Carbon and Low-Alloy Steels [S. V. Kovalenko, V. I. Kuchkin, et al.; <i>IZVESTIYA VYSSHIKH UCHEBNYKH ZAVEDENIY: CHERNAYA METALLURGIYA</i> , Feb 91]	2
Developing and Studying the Technology of Die Rolling Workpieces Used to Make Hydrocylinders [V. D. Shalayev, N. A. Koryakin, et al.; <i>KUZNECHNO-SHTAMPOVOCHNOYE PROIZVODSTVO</i> , Dec 90]	2
Die Rolling. Current and Future Potential [N. A. Koryakin; <i>KUZNECHNO-SHTAMPOVOCHNOYE PROIZVODSTVO</i> , Dec 90]	2
Low-Scrap Production of Draftless Forgings at the Kopey Machinery Plant [M. M. Chernykh, P. G. Tyrsin, et al.; <i>KUZNECHNO-SHTAMPOVOCHNOYE PROIZVODSTVO</i> , Dec 90]	3
Estimating the Size of Semi-Finished Products Swaged During the Production of Draftless Forgings [M. M. Chernykh, S. A. Puchin, et al.; <i>KUZNECHNO-SHTAMPOVOCHNOYE PROIZVODSTVO</i> , Dec 90]	3
Hydraulic Lever Shears [G. P. Poltavtsev et al.; <i>KUZNECHNO-SHTAMPOVOCHNOYE PROIZVODSTVO</i> , Dec 90]	3
More Refined Mathematical Models of Forging Press Mechanisms [V. M. Smolyaninov, Ye. D. Machekhina, et al.; <i>KUZNECHNO-SHTAMPOVOCHNOYE PROIZVODSTVO</i> , Dec 90]	3
Four-Way Press Forging of Continuously Cast Special Alloy Steels [V. A. Lazorkin, V. A. Tyurin, et al.; <i>KUZNECHNO-SHTAMPOVOCHNOYE PROIZVODSTVO</i> , Dec 90]	4
Use of Limiting Friction Laws to Improve Metal Forming Processes [A. N. Levanov; <i>KUZNECHNO-SHTAMPOVOCHNOYE PROIZVODSTVO</i> , Dec 90]	4
Results From Performance Tests of a Two-Zone Forging Furnace [F. Z. Sabrikov, Yu. P. Filatov, et al.; <i>KUZNECHNO-SHTAMPOVOCHNOYE PROIZVODSTVO</i> , Dec 90]	4
Processes for Deep-Drawing Conically Shaped Parts [V. I. Kazachenok, Yu. O. Mikhaylov, et al.; <i>KUZNECHNO-SHTAMPOVOCHNOYE PROIZVODSTVO</i> , Dec 90]	5
Spin-Forming Thin Flat Parts Embossed on One Side [Ya. N. Duka, V. B. Fedorov, et al.; <i>KUZNECHNO-SHTAMPOVOCHNOYE PROIZVODSTVO</i> , Dec 90]	5
Structure and Strength of Spun-Formed Tube [A. P. Nishta, Ye. L. Korobeynikova, et al.; <i>KUZNECHNO-SHTAMPOVOCHNOYE PROIZVODSTVO</i> , Dec 90]	5
Influence of Repeated Hardening on Microstructure and Mechanical Properties of ShKh15 Steel [B. I. Maksumov, I. O. Khazanov; <i>IZVESTIYA VYSSHIKH UCHEBNYKH ZAVEDENIY: CHERNAYA METALLURGIYA</i> , Feb 91]	5
Chill Casting of High-Strength Cast Iron Body Parts [L. A. Solntsev, V. D. Shifrin, et al.; <i>LITEYNOYE PROIZVODSTVO</i> , Feb 91]	6

Status and Prospects for Development of Precision Casting in Lined Chill Mold [V. M. Koshevatskiy, S. B. Kantor, et al.; LITEYNOYE PROIZVODSTVO, Feb 91]	6
Reaction of Hydrogen With Ti <sub>4</sub> Fe Alloys [V. N. Verbetskiy, R. R. Kayumov, et al.; IZVESTIYA AKADEMII NAUK SSSR: SERIYA METALLY, Jan 91]	6
X-Ray Measurement of Residual Stresses in Thin TiN Coatings [S. Ya. Betsofen, L. M. Petrov; IZVESTIYA AKADEMII NAUK SSSR: SERIYA METALLY, Jan 91]	6
Properties of Crystallitons Upon Superplastic Deformation of Fine-Crystalline Materials [V. M. Greshnov; IZVESTIYA AKADEMII NAUK SSSR: SERIYA METALLY, Jan 91]	7
Structure and Phase Composition of Contact Zones of Bimetals Produced by Explosive Welding [N. V. Popova, V. Z. Kutsova, et al.; IZVESTIYA AKADEMII NAUK SSSR: SERIYA METALLY, Jan 91]	7
Phase Composition and Properties of Nickel Casting Alloy With Variable Titanium and Aluminum Content [V. D. Kireyev, N. V. Kolyasnikova, et al.; IZVESTIYA AKADEMII NAUK SSSR: SERIYA METALLY, Jan 91]	7
Change in Structure of Iron and Steel Upon Very Deep Penetration of High-Velocity Particles [S. M. Usherenko, S. I. Gubenko, et al.; IZVESTIYA AKADEMII NAUK SSSR: SERIYA METALLY, Jan 91]	7
Plastic Deformation of Polycrystalline Beryllium at 400-850 K [V. P. Zharinov, A. N. Pavlychev; IZVESTIYA AKADEMII NAUK SSSR: SERIYA METALLY, Jan 91]	7
Kinematic Models Considering Nonuniformity of Deformation in Rolling [Yu. I. Kamenshchikov, L. A. Barkov, et al.; IZVESTIYA AKADEMII NAUK SSSR: SERIYA METALLY, Jan 91]	8
Thermodynamic Specifics of Steel Refining With Blowing of Silicocalcium Powder [A. G. Tyurin, G. G. Mikhaylov; IZVESTIYA AKADEMII NAUK SSSR: SERIYA METALLY, Jan 91]	8
Problems of Heating Furnace Automatic Process Control System Design [Ye. V. Toropov, V. I. Panferov; IZVESTIYA VYSSHIKH UCHEBNYKH ZAVEDENIY: CHERNAYA METALLURGIYA, Feb 91]	8
Local Morphology of Graphitized Steel Hardened With Induction Heating [G. A. Berlin, V. M. Zhurakovskiy, et al.; IZVESTIYA VYSSHIKH UCHEBNYKH ZAVEDENIY: CHERNAYA METALLURGIYA, Feb 91]	8
$\alpha \rightarrow \alpha''(\alpha')$ Conversion in VT30 Titanium Alloy Upon Plastic Deformation [M. V. Maltsev; IZVESTIYA AKADEMII NAUK SSSR: SERIYA METALLY, Jan 91]	9

## NONFERROUS METALS, ALLOYS, BRAZES, SOLDERS

Stressed State of Carbide Phase of BK6 Hard Alloy During Pulsed Laser Treatment [A. G. Grigoryants, S. I. Yaresko; Kiev SVERKHTVERDYIE MATERIALY No 2, Jan 91]	10
Effect of Ultradispersed Diamond-Like Carbon Phase Particles on Microstructure of Electrodeposited Chromium Coating [A. L. Vereshchagin, I. I. Zolotikhina, et al.; SVERKHTVERDYIE MATERIALY No 2, Jan 91]	10
Cold Compacting of CNB Powders at High Pressures [O. N. Andreyev, N. P. Bezhenar; SVERKHTVERDYIE MATERIALY No 2, Jan 91]	10
Effect of Surface Chemical Composition of Synthetic Diamond Micropowders on Polycrystals Sintered From Them [V. G. Alishin, A. A. Smekhnov, et al.; SVERKHTVERDYIE MATERIALY No 2, Jan 91]	11
Hardness and Cracking Resistance of Materials Based on Dense BN Modifications [S. N. Dub, A. I. Ignatusha; SVERKHTVERDYIE MATERIALY No 2, Jan 91]	11
High-Temperature Strength of Polycrystalline Boron Nitride With Titanium Nitride-Based Binder [I. M. Androssov, V. T. Vesna, et al.; SVERKHTVERDYIE MATERIALY No 2, Jan 91]	11
Studying the Stressed State of Elboron-P Polycrystals [V. A. Pesin, Ya. I. Kunin, et al.; SVERKHTVERDYIE MATERIALY No 2, Jan 91]	12
Change in the Impurity Composition of Synthetic Diamond Single Crystals During P-T Treatment [V. G. Malogolovets, G. V. Chipenko, et al.; SVERKHTVERDYIE MATERIALY No 2, Jan 91]	12
Effect of Trap Energy Structure on Injection Properties of Contacts on a Synthetic Diamond [L. A. Romanko, A. G. Gontar; SVERKHTVERDYIE MATERIALY No 2, Jan 91]	12
Autoradiographic Study of Diamond Crystals and Carbide Phases [A. A. Putyatin, V. I. Korobkov, et al.; SVERKHTVERDYIE MATERIALY No 2, Jan 91]	13

Use of Ultrafine-Grain Aluminum Alloys in Crucial Design Parts [M.Kh. Rabinovich and M.V. Markushev; TSVETNYYE METALLY, Dec 90]	13
Effect of Annealing Practice on the Properties of Copper-Clad Aluminum Wire [B.M. Zhukov and V.I. Romanovskiy; TSVETNYYE METALLY, Dec 90]	13
Problems of Establishment of Small Specialized Enterprises in the Industry Engaged in Working and Processing of Nonferrous Metals and Alloys [G.N. Strakhov; TSVETNYYE METALLY, Dec 90]	14
Defect Formation During Growth of Silicon Multilayer Epitaxial Composites [P.N. Galkin, O.P. Golovko, V.P. Tokarev, et al.; TSVETNYYE METALLY, Dec 90]	14
Factors Affecting the Quality of Protective Coatings on Magnesium [A.Ye. Stolina and V.I. Gribov; TSVETNYYE METALLY, Dec 90]	14
Development of Automation Systems for Lead and Zinc Production Processes on the Basis of Noise-Proof Algorithms [Yu.M. Abdeyev, V.V. Terekhin, and G.K. Shadrin; TSVETNYYE METALLY, Dec 90]	15
Autogenous Lead Production Method in the KIVtSET-TsS Unit [A.P. Sychev, I.P. Polyakov, Yu.A. Grinin, et al.; TSVETNYYE METALLY, Dec 90]	15
Structure and Properties of Aluminum-Copper Welded Joints [T.M. Mozhanskaya and N.T. Chekanova; METALLOVEDENIYE I TERMICHESKAYA OBRABOTKA METALLOV, Dec 90]	15
Heat Treatment of Aluminum Bronzes Exhibiting Shape-Memory Effect [M.A. Kravchenko, V.K. Larin, and S.G. Radchenko; METALLOVEDENIYE I TERMICHESKAYA OBRABOTKA METALLOV, Dec 90]	16

## NONMETALLIC MATERIALS

Mechanism of Optical Glass Polishing by "Akvapol" Tool [V. V. Rogov; SVERKHTVERDYIE MATERIALY, No 6, 1990]	17
Paranite-New Material for Solid-Phase High-Pressure Equipment Containers and Seals [Z. Raab, K. Volshtet, et al.; SVERKHTVERDYIE MATERIALY, No 6, 1990]	17

## PREPARATIONS

Technology for Producing a Heat-Resistant Alloy [V. A. Brovko, A. I. Smirnov, et al.; LITEYNOYE PROIZVODSTVO, Dec 90]	18
Antimony-Based Alloys for Composite Materials [Yu. I. Rubenchik, I. A. Solovyev, et al.; LITEYNOYE PROIZVODSTVO, Dec 90]	18
Influence of Silicon on Properties of Nearly Eutectic Iron [L. S. Volkovich, B. E. Kletskin; LITEYNOYE PROIZVODSTVO, Dec 90]	18
Making Fusion-Cast Channels for MDN-6A Magnetohydrodynamic Metering Devices [V. N. Moiseyenko, O. M. Drobot, et al.; LITEYNOYE PROIZVODSTVO, Dec 90]	18
Automatic Metering Control in an Electric Furnace Equipped With a Submersible Magnetohydrodynamic Pump [Yu. A. Krylov, V. I. Ruskol, et al.; LITEYNOYE PROIZVODSTVO, Dec 90]	19
Casting Finishing Operations at the Volga Automotive Plant [S. I. Vasilyev, A. G. Negulyayev, et al.; LITEYNOYE PROIZVODSTVO, Dec 90]	19
Finishing Operations at Minavtoselkhoz mash Foundries [I. A. Yaskovich; LITEYNOYE PROIZVODSTVO, Dec 90]	19
Cryogenic Treatment of Castings [G. M. Kimstach, B. M. Drapkin, et al.; LITEYNOYE PROIZVODSTVO, Dec 90]	20

## WELDING, BRAZING, SOLDERING

Brittle Failure in Steels With Developed Crystal Textures [V. S. Girenko, A. V. Bernatskiy, et al.; AVTOMATICHESKAYA SVARKA, Jan 91]	21
Improving the Induction Hard-Facing of Thin Shaped Disks [Ch. V. Pulka, O. N. Shabliy, et al.; AVTOMATICHESKAYA SVARKA, Jan 91]	21
Capacitor-Discharge Welding and Mechanical Properties of Aluminum Alloy Fasteners [D. M. Kaleko, N. A. Chvertko; AVTOMATICHESKAYA SVARKA, Jan 91]	21
Using an Electromagnetic Sprayer to Apply Coatings [A. I. Ponomarev, B. V. Danilchenko, et al.; AVTOMATICHESKAYA SVARKA, Jan 91]	21
Temperature Field and Phase Composition of Metal in the Heat-Affected Zone During Underwater Welding [S. F. Budz, B. D. Drobenko, et al.; AVTOMATICHESKAYA SVARKA, Jan 91]	22

Effect of Load Frequency on Steel and Weld Fatigue Resistance [V. S. Kovalchuk; AVTOMATICHESKAYA SVARKA, Jan 91]	22
Controlling Metal Transfer With Pulsed MIG Welding [V. Senchak, P. Orsag; AVTOMATICHESKAYA SVARKA No 1, Jan 91]	23
Estimating the Effect of Residual Stresses on Low-Cycle Weld Fatigue [V. I. Makhnenko, R. Yu. Mosenkis; AVTOMATICHESKAYA SVARKA, Jan 91]	23
Holographic Measurement of Residual Stresses in Butt-Welded 12Kh2N4MD Steel [L. M. Lobanov, V. A. Pivtorak, et. al.; AVTOMATICHESKAYA SVARKA, Jan 91]	23
Stress Distribution Along Fillet-Welded T-Joints Between Elements of Limited Rigidity [V. I. Makhnenko, Ye. A. Velikoivanenko, et. al.; AVTOMATICHESKAYA SVARKA, Jan 91]	24

## MISCELLANEOUS

A Hydrodynamic Theory of Mass Transfer Anomaly in Solid Bodies Subjected to Shock [B. V. Yegorov, L. O. Zvorykin, et al; METALLOFIZIKA, Jan 91]	25
Linear Creep Limit in One- and Two-Dimensional Aluminum Polycrystals [Ye. Ye. Badiyan, V. B. Rabukhin, et al.; METALLOFIZIKA, Jan 91]	25
Thermal Conductivity of Berillium as a Function of Temperature Between 15 and 275 K [S. A. Guzhva, F. F. Lavrentyev, et al.; METALLOFIZIKA, Jan 91]	25
Certain Features of $\gamma$ -Fe Crystal Formation in Fast-Quenched $\text{Fe}_{85}\text{B}_{15}$ Alloy [A. P. Brovko, L. Ye. Mikhaylova, et al.; METALLOFIZIKA, Jan 91]	25
Monitoring of Operation of the Drives of Pulsating-Bottom Furnaces [T.A. Vorobyeva and L.F. Liberman; METALLOVEDENIYE I TERMICHESKAYA OBRABOTKA METALLOV, Dec 90]	26
A One-Dimensional Model of Thin-Film Growth [A. V. Osipov; METALLOFIZIKA, Jan 91]	26
Magnetoelastic Effects in Weakly Ferromagnetic Alloys [A. A. Povzner, A. G. Volkov; METALLOFIZIKA, Jan 91]	26
New Refractory Compositions for Closing of Iron Notches and Ramming of Runners [V. M. Gorobitsov, V.N. Belyakov, V.F. Sereda, et al.; METALLURG, Dec 90]	27
The Future of Sheet and Plate Production [Yu. D. Zheleznov; METALLURG, Dec 90]	27
Will Fines Protect the Environment? [I. Dnepryanko and A. Simagov; METALLURG, Dec 90]	27

**Reduction of Deformation of Cylindrical Parts During Nitriding**

917D0115D Moscow METALLOVEDENIYE I  
TERMICHEKSKAYA OBRABOTKA METALLOV  
in Russian No 12, Dec 90 pp 18-19

[Article by I.S. Dukarevich]

UDC 621.785.532:620.192.47

[Abstract] A general discussion of warping of nitrided parts as a result of volume changes of the surface layer is presented along with ways of minimizing it (nitriding only the working surfaces, increasing the part thickness, correct sequence of machining and heat treatment operations, and increasing the nitride layer uniformity by phosphating prior to nitriding) is presented. A new way of minimizing warping is described. It consists of protecting strips of the surfaces from nitriding by tinplating these strips. This produces an interrupted nitride layer and reduces the residual compressive stresses, thus minimizing warping. In one example warping of a steel ring was reduced from 5.17 mm to 3.46-3.77 mm and 2.33mm by tinplating of strips covering, respectively, 21 percent and 55 percent of the outside surface. One figure; one table; two Russian references.

**Effect of Heat-Treatment Practice on Brittle-Fracture Resistance of Heavy-Plate Low-Alloy Steel 09G2S**

917D0115 Moscow METALLOVEDENIYE I  
TERMICHEKSKAYA OBRABOTKA METALLOV  
in Russian No 12, Dec 90 pp 2-5

[Article by V.M. Gornitskiy, G.R. Shneyderov, and T.G. Zaytseva, TsNIIPROYEKTSTALKONSTRUKTSIYA (Central Scientific-Research and Design Institute of Metal Structures)]

UDC 21.785.7:9.14.018.298

[Abstract] At the Novolipetsk Metallurgical Combine the blast-furnace shells made of 50-mm thick normalized plates of steel 09G2S (0.08% C, 1.5% Mn, 0.1% Cr, 0.23% Ni, 0.018% S, 0.21% P) develop long cracks in cold weather. Their semibrittleness temperature is as high as 35 °C. Oil-quenching was found to greatly increase the impact toughness but has little effect on strength properties of steel 09G2S. Water-quenching and tempering at 600 to 650 °C was found to give a structure consisting of tempered sorbite and polygonal ferrite, which results in the best combination of ductility and strength. The recommended heat treatment for 40 to 50 mm plates for used in parts of blast furnace shells that are not water cooled consists of water-quenching and tempering at about 630 °C. This produces a 0.2 offset yield strength of 400 N/mm<sup>2</sup>, a minimum ultimate tensile strength of 530 N/mm<sup>2</sup>, an elongation of 27%, an area reduction of 75%, and a semibrittleness temperature of -20 °C. Figures 5; table 1; 2 Russian references.

**Use of Water Solution of Technical Lignosulfonate for Quenching Heavy Steel Articles**

917D0115B Moscow METALLOVEDENIYE I  
TERMICHEKSKAYA OBRABOTKA METALLOV  
in Russian No 12, Dec 90 pp 5-10

[Article by V.Ye. Loshkarev, L.I. Sorokina, and S.A. Peskishev, NPO TsKTI (Scientific-Production Association) Central Scientific-Research and Design Boiler and Turbine Institute imeni I.I. Polzunov and the Bolshevik Plant]

UDC 621.78.063

[Abstract] Quenching efficiency of lignosulfonate solutions in water at concentrations between 6.5 and 40 percent was studied in order to determine whether lignosulfonate solutions can be used for quenching heavy sections, such as rotors and rolling-mill rolls, of chromium-alloyed steels. The criteria used for evaluation of quenching efficiency were the time required to cool the center of the workpiece to 300 °C and the maximum internal stresses produced by quenching. It was found that in the case of workpieces thinner than 200 mm a 6.5-percent lignosulfonate solution can replace oil as quenching medium; a 12-percent solution can replace oil in the case of thicker workpieces. Prequenching in water followed by final quenching in oil can be replaced by quenching in a 12-percent lignosulfonate solution in the case of workpieces thicker than 500 mm. Lignosulfonate solutions can not replace water as quenching medium because their cooling rate is too low, but they can be used for final quench after a preliminary water quench in order to increase the hardenability of rolls. The cooling rate of 26- and 40-percent lignosulfonate solutions was found to be too low for them to be used as replacements for oil or water. Figures 5; 1 table; references 8, 1 Western, 7 Russian.

**Ion Nitriding of Steel Kh12F1**

917D0115C Moscow METALLOVEDENIYE I  
TERMICHEKSKAYA OBRABOTKA METALLOV  
in Russian No 12, Dec 90 pp 15-17

[Article by A.I. Slosman and N.M. Lemeshev, Tomsk Polytechnic Institute]

UDC 621.785.532.062.57:669.11526.194

[Abstract] Stamping-tool steel Kh12F1 was nitrided at 475 to 575 °C in cracked ammonia in a previously described glow-discharge plasma unit after annealing, quenching, quenching and tempering, and quenching and chilling in liquid nitrogen. This produced a surface hardness of 1150 to 1250 H. The nitriding time between 3 and 300 minutes has almost no effect on surface hardness of annealed specimens, and some softening (due to tempering effect of nitriding temperature) was observed in the case of quenched specimens. Increased

nitriding temperature leads to noticeable softening due to tempering and coagulation of the nitride phase. The nitrided layer thickness increases with nitriding temperature and time and with increasing quenching temperature (between 850 and 1250 °C). Tempering and chilling in nitrogen have little effect on the nitrided layer thickness. Prior heat treatment has little effect on the wear of nitrided specimens. A combination of high surface hardness and strength requires quenching before nitriding. Maximum surface hardness is obtained by quenching from 1250 °C and chilling in nitrogen prior to nitriding. Quenching and high-temperature tempering prior to nitriding is recommended in order to obtain high wear resistance and dimensional stability. Figures 5 (Figures 1 and 2 are on inside back cover); 4 Russian references.

#### **Influence of Calcium and Barium Modification on Microstructure of Carbon and Low-Alloy Steels**

917D0145C Moscow IZVESTIYA VYSSHIKH  
UCHEBNIKH ZAVEDENIY: CHERNAYA  
METALLURGIYA in Russian Feb 91 pp 55-58

[Article by S. V. Kovalenko, V. I. Kuchkin, V. S. Kovalenko, Donetsk Polytechnical Institute]

UDC 669.15'891'893-194:539.24/.27

[Abstract] Steels types St3p, 45, 15G2S and 25G2S were studied, made in a laboratory 60 kg induction furnace and poured in 20 kg capacity molds. The tendency toward austenite grains both were studied at 900-1200°C, holding time 15 minutes, with specimens quenched in water then etched in saturated sodium picrate. Low-temperature ferrite recrystallization tendency was determined by the double hardness method in the carbon steel. It was found that calcium and barium significantly reduce the austenite and true grain size in the carbon and low-alloy steels tested. The tendency toward low-temperature recrystallization is virtually unchanged by the modification. Calcium and barium increased the dispersion and density of pearlite in hot rolled steel and facilitate more uniform distribution of austenite decomposition products. Figures 3; References 6: Russian.

#### **Developing and Studying the Technology of Die Rolling Workpieces Used to Make Hydrocylinders**

917D0128D Moscow  
KUZNECHNO-SHTAMPOVOCHNOYE  
PROIZVODSTVO in Russian No 12, Dec 90 pp 7-8

[Abstract of article by V. D. Shalayev, N. A. Koryakin, V. P. Glukhov, Ye. I. Gurevich; Izhev Mechanical Institute]

UDC 621.774.25.001.2

[Abstract] The use of the die rolling process to make the workpieces from which hydrocylinders are manufactured was studied. The workpieces were made on

hydraulic presses with a rated force of 3000 to 4000 kN. The presses were equipped with die rolling tooling, the components and functions of which were described and illustrated. The starting blanks were made from turned hot-rolled tubing made from heat-treated 35Kh steel. The tubing was 102 mm in diameter and had a wall thickness of 17 mm. The first step in making the semi-finished product involved crimping the end of the workpiece in the die to form a collar to facilitate the action of the mandrel. During the second and third steps, deformation was accomplished in 2 to 5-mm increments per die rolling cycle. Wall thickness was reduced by 39% and 41%, respectively, with total deformation equalling 64%. Cold-drawn tubing, cup-shaped forgings, and rolled product with machined cavities could also be used as starting blanks. Wall thickness could be reduced 60-65% per pass. The possibility of die rolling workpieces without pre-machining the original blanks was also studied. This was found to be feasible when the amount and degree of deformation per pass were increased. Both parameters were equally effective in reducing variations in wall thickness (by 27-51%) and the amount of play in the workpiece axis and in improving tolerances. This die rolling method saves 25% on labor and reduces metal consumption by increasing the metal utilization coefficient 1.5 to 3-fold. Also, due to strain-hardening in spun-formed parts, low-alloy and carbon steels can be used in place of alloy steels. Figures 2; references 2: Russian.

#### **Die Rolling. Current and Future Potential**

917D0128C Moscow  
KUZNECHNO-SHTAMPOVOCHNOYE  
PROIZVODSTVO in Russian No 12, Dec 90 pp 5-7

[Abstract of article by N. A. Koryakin, Izhev Mechanical Institute]

UDC 621.774.25.001

[Abstract] Current and potential applications of the die rolling process were briefly summarized. This process, which can be effected on conventional forging presses, is becoming more versatile as a result of being able to impart an oscillating motion to the mandrel, die, or workpiece. The mandrel, or forming tool, can have any of a number of shapes varying from the simplest types of flat and tapered shapes to more complex conical and mating shapes. The dies are flat, conical, or cylindrical. Die rolling can be used to prepare workpieces and to manufacture semi-finished and finished products. Examples of all three applications were provided. New applications of this process have been used to reduce costs and save metal. The Izhev Mechanical Institute has developed base models of die rolling equipment, including a rotary equipment line and powerful presses with up to 10 Mn of force. This equipment has been used to make 20 different types of complex precision parts. In order for the die rolling process to become widely

adopted, production models of die rolling equipment must be developed. Figures 4, tables 1; references 5: Russian.

### Low-Scrap Production of Draftless Forgings at the Kopey Machinery Plant

917D0128B Moscow

KUZNECHNO-SHTAMPOVOCHNOYE

PROIZVODSTVO in Russian No 12, Dec 90 pp 3-5

[Abstract of article by M. M. Chernykh, P. G. Tyrsin, V. A. Privalov, L. A. Mamontova, A. I. Pyankov; Izhev Mechanical Institute]

UDC 621.73.043

[Abstract] Researchers at the Kopey Machinery Plant have developed mathematical formulas for calculating forging parameters for the production of ringed, bossed, and bossed lug forgings. The formulas were derived from tests carried out to determine how variations in the length ( $h_p$ ) of one section of the lateral surface of finished cylindrical forgings affected the value of the maximum deviation ( $\Delta r_{max}$ ) of the lateral surface profile from a line corresponding to the diameter of the final shaping part of the die,  $D_k$ . Rectangular steel test specimens 20 to 45 mm in height, with wall thicknesses from 10 to 35 mm, were forged in tapered dies lubricated with a machine oil and graphite mixture. The contour slope and draft angles were equal. The neutral diameter,  $D_n$ , was set at 79.4 mm. The length of the section in question was varied within a range of  $0 < h_p/D_n < 0.23$ . The results indicated that the upper boundary for  $h_p$  should be approximately equal to  $0.12 D_n$ . Equations were recommended for calculating the nominal values for  $h_p$  and the values for  $\Delta r_{max}$ , and semi-finished forging height and wall thickness. These formulas were applied to the production of draftless forgings and resulted in a reduction in metal consumption of 100 to 150 kg per ton of forgings. Figures 4, tables 1; references 3: Russian.

### Estimating the Size of Semi-Finished Products Swaged During the Production of Draftless Forgings

917D0128A Moscow

KUZNECHNO-SHTAMPOVOCHNOYE

PROIZVODSTVO in Russian No 12, Dec 90 pp 2-3

[Abstract of article by M. M. Chernykh, S. A. Puchin, V. N. Gorbunov, V. A. Privalov, F. G. Yaylenko; Izhev Mechanical Institute]

UDC 621.73.043

[Abstract] Shear strain occurring in the outer facial edge of semi-finished work swaged to produce draftless forgings was determined experimentally as a function of relative specimen height and internal diameter, draft, and the slope of the tapered part of the swaging die. The specimens were made of lead and 45 steel. The smaller

external diameter of the steel specimens was accepted as equal to 79.4 mm. A planning matrix was used to calculate the other dimensions. Before swaging, the specimens were induction heated to a temperature of  $1170 \pm 20K$ , which was recorded by an FPP-4 semiphotovoltaic pyrometer. The specimens were swaged on a crank-driven trimming press with 2.5 MG of force in dies made from 5KhNM steel, the faces of which were lubricated with a mixture of machine oil and graphite. The results were presented as first degree polynomials in the form of a partial quadratic equation and successfully used to develop a more efficient swaging process. An example of the steps and equations used to estimate the size of the swaged forgings was provided. Figures 2, tables 3; references 4: Russian.

### Hydraulic Lever Shears

917D0128L Moscow

KUZNECHNO-SHTAMPOVOCHNOYE

PROIZVODSTVO in Russian No 12, Dec 90 p 27

[Abstract of article by G. P. Poltavtsev]

UDC 621.967.1

[Abstract] The Azov Donpressmash Production Association has developed an experimental hydraulic lever shear station for the precision cutting of measured lengths of rolled product. It consists of a base on which the lower contoured blade and clamp are mounted, and a beam on which the upper contoured blade and clamp are mounted. The beam is powered by a hydraulic cylinder built into the base. The rolled product is placed in the proper sized aperture formed by the mating blades, secured by the clamps, and cut by the oscillating motion of the beam. Billet length is controlled by a movable stop. Equipment specifications are provided. Using the machine would save 30,000 rubles annually. Figures 2.

### More Refined Mathematical Models of Forging Press Mechanisms

917D0128K Moscow

KUZNECHNO-SHTAMPOVOCHNOYE

PROIZVODSTVO in Russian No 12, Dec 90 pp 25-26

[Abstract of article by V. M. Smolyaninov, Ye. D. Machekhina, V. I. Gusinskiy]

UDC 621.979.134.001

[Abstract] The Experimental Scientific Research Institute of Forging Machinery developed a method for refining mathematical models of forging press mechanisms that factor in operating load, actual distribution of link mass, and force of friction in each kinematic pair. Application of the method was demonstrated by creating a mathematical model for crank-and-rocker/slide mechanisms. A software package consisting of the basic model and a graphics output program was written for Apricot



personal computers. This method can be used to improve the design of forging machinery. Figures 4; references 2: Russian.

#### Four-Way Press Forging of Continuously Cast Special Alloy Steels

917D0128J Moscow

KUZNECHNO-SHTAMPOVOCHNOYE

PROIZVODSTVO in Russian No 12, Dec 90 pp 16-18

[Abstract of article by V. A. Lazorkin, V. A. Tyurin, Yu. N. Skorniyakov, T. V. Kurashova, V. A. Kulikov]

UDC 621.73.01

[Abstract] The feasibility of interposing forging equipment between continuous casting machines and final rolling mills was studied. Test 65Kh13 and 8Kh4V9F2 (EI 347) steels were made in a 400-kg induction furnace and cast into billets 160 mm in diameter on a horizontal continuous casting machine. The billets were then forged using 5 MN of force on a specially equipped four-way press. A specific ratio of contact friction conditions was assigned to the working surfaces of the dies during the forging operation. In this way, it was possible to both apply compressive stresses to the surface of the work and to induce the penetration of intensive plastic deformation into the axial zone of the workpiece. During the first pass, the metal was allowed to flow into the spaces between the die faces. Each subsequent pass yielded a forging with a square cross-section (reduction coefficient of 2.2), while macroshears were induced. After metallographic cross-sections were cut from the forgings, they were reformed on a press in flat dies to produce forgings with a 45x45-mm cross-section (reduction coefficient of 3.5). The forgings were of consistently high quality throughout their cross-section, and there were no surface ruptures, even with a reduction coefficient as low as 2.2. This information was used to develop a casting and forging line to produce special and alloy steel workpieces for rolling, as well as various types of forgings. The line will be computer controlled and set up to handle any desired combination of steel, workpiece, and end product. The benefits of adopting this technology include a 2-fold drop in energy consumption, a 2 to 2.5-fold increase in labor productivity, lower capital expenditures to modernize forging shops, and a 20 to 30% reduction in the amount of steel consumed to produce one ton of final product. Figures 2.

#### Use of Limiting Friction Laws to Improve Metal Forming Processes

917D0128I Moscow

KUZNECHNO-SHTAMPOVOCHNOYE

PROIZVODSTVO in Russian No 12, Dec 90 pp 13-16

[Abstract of article by A. N. Levanov]

UDC 621.73.001

[Abstract] The results of systematic studies of contact friction occurring during metal forming operations were presented. The studies were carried out by the Department of Metal Forming of the Ural Polytechnic Institute. The first part of the article discusses the statement of the problem. The second part generalizes the experimental data gathered during studies of the contact and interlayer stresses generated during various processes. The third part of the article is an exposition of the general laws of limiting friction. The last part of the article discusses how this knowledge can be applied to improve metal forming operations and friction testing. Recommendations are based on using self-adjusting tooling in dynamic processes and on the utilization of active friction forces during upsetting and die-forging. A new closed-die forging technique that uses self-adjusting dies to compensate for excess metal was described. Figures 3; references 15: Russian.

#### Results From Performance Tests of a Two-Zone Forging Furnace

917D0128H Moscow

KUZNECHNO-SHTAMPOVOCHNOYE

PROIZVODSTVO in Russian No 12, Dec 90 pp 12-13

[Abstract of article by F. Z. Sabrikov, Yu. P. Filatov, G. V. Kopytov; Izhev Mechanical Institute]

UDC 621.733:621.783.2.002

[Abstract] Tests were performed to measure temperature equalization in workpieces reheated in an MPC 5-ton forging furnace and the temperature inside the furnace during reheating. Three KhA thermocouples were implanted in a test bloom at depths of 50, 110, and 170 mm. Portable PPR platinum/platinum-rhodium thermocouples and an optical pyrometer were also used to measure bloom temperature. Reheating time was 5 hours and 20 minutes from the time the test bloom entered the furnace until it was discharged. The temperature inside the furnace during reheating did not exceed 1370°C. The temperature of the workpiece surface reached 1150°C. The temperature inside the furnace reached 1280-1300°C in the heating zone, and 1220-1240°C in the soaking zone. Furnace productivity, allowing for downtime, was 4.62 tons per hour, or 126% of rated productivity. Without allowing for downtime, but factoring in dinner and rest breaks, productivity was 51.6 forgings per hour, or 160% of rated capacity. Average gas consumption was 249 sq m. Using these heating parameters, the fuel, which is 10% CO<sub>2</sub> and 3.2% O<sub>2</sub>, burns completely. The air-fuel ratio was 1.13, and stack gas pressure was +1.96 Pa. Figures 3, tables 1.

**Processes for Deep-Drawing Conically Shaped Parts**

917D0128G Moscow  
KUZNECHNO-SHTAMPOVOCHNOYE  
PROIZVODSTVO in Russian No 12, Dec 90 pp 10-12

[Abstract of article by V. I. Kazachenok, Yu. O. Mikhaylov, T. V. Sabrikova, V. A. Sandrov; Izhev Mechanical Institute]

UDC 621.7.079

[Abstract] Theoretical analyses of hydroforming and a combined deep-drawing and bulging process were performed using experimental data in order to determine the most suitable applications for each process. Hydroforming was found to work best when making conically shaped parts with a relatively low profile from a flat workpiece. The operation is performed in dies with simple shapes on universal machines, using industrial oil or a water-oil emulsion with a viscosity of no more than 2.7 P. This process, by greatly decreasing the amount of metal deformed without being in contact with the punch and by developing active friction forces where the punch and blank come in contact, reduces stresses in the vulnerable part of the blank and blank-die friction losses. As a result, the degree of deformation can be increased while decreasing the probability that the blank will give way during forming. The combined deep-drawing and bulging process was found to be more suitable for making conically shaped parts with a relatively high profile. The first step in making these parts is the same as in the conventional process and entails forming a cylindrical workpiece. However, instead of using separate operations to taper and flange the bottom of the part, drawing of the bottom section and bulging of the conical flange are commenced simultaneously. This has the effect of transferring the bulging force to the cylindrical part of the workpiece, thereby creating a tapering zone and reducing the length of the drawn section. This in turn reduces tensile stresses in the vulnerable part of the workpiece and increases the degree of deformation possible per operation. A process combining hydroforming and the deep-drawing/bulging operation was also developed for making "Konus" parts from 10kp steel strip. All three processes reduce the number of operations required to make a part and increase labor productivity. Figures 5, tables 1; references 3: Russian.

**Spin-Forming Thin Flat Parts Embossed on One Side**

917D0128F Moscow  
KUZNECHNO-SHTAMPOVOCHNOYE  
PROIZVODSTVO in Russian No 12, Dec 90 p 9

[Abstract of article by Ya. N. Duka, V. B. Fedorov, A. B. Krylov; Izhev Mechanical Institute]

UDC 621.983.002

[Abstract] A process was developed for spin-forming thin flat parts embossed on one side. The parts are made from blanks of 10-grade steel 1.5 mm thick on a model PO440 hydraulic press equipped with spin-forming tooling. After the blanks are cleaned and lubricated, they are subjected to the initial spin-forming process to form the preliminary pattern on the workpiece. At this stage, process force (P) is 3 MN, the spin angle ( $\phi$ ) is 0.035 radians, and the number of cycles (n) is 5-7. The preliminary pattern is set at angle  $\phi$ , the size of which depends on  $\phi$  and n during the second forming step. They are then annealed, relubricated and washed, and spun-formed a second time to produce the finished piece (P = 3.5 MN,  $\theta = 0.035$ , n = 8-10). The two-step process makes it possible to emboss thin workpieces without causing dimpling. Using spin-forming instead of machining to emboss thin flat parts reduces the per-part cost by 10 rubles. Figures 2; references 2: Russian.

**Structure and Strength of Spun-Formed Tube**

917D0128E Moscow  
KUZNECHNO-SHTAMPOVOCHNOYE  
PROIZVODSTVO in Russian No 12, Dec 90 pp 8-9

[Abstract of article by A. P. Nishta, Ye. L. Korobeynikova, M. B. Zinovyeva, Ye. I. Gurevich; Izhev Mechanical Institute]

UDC 621.774.002

[Abstract] A study was carried out to determine the effectiveness of using a spin-forming process to make cylindrical articles from heat-treated 35Kh steel. Cylinders 90 mm in diameter were made conventionally and with the new process. The conventional technology includes oil-quenching from 860°C, tempering at 570°C, and machining. The first two steps of the experimental process are the same, but after tempering, the workpiece is spun-formed and then annealed at 570°C to effect polygonization. Holding time is 30 minutes during quenching and 2 hours during tempering and annealing. The new process makes it possible to accomplish extensive plastic deformation without having to reanneal the workpiece. Significant strain hardening of the metal occurs, while plasticity and ductility remain high. The structure of the metal consists of directional microstructure of highly annealed martensite and a fragmented substructure and is more resistant to brittle failure and cracking. Use of this process increases the metal utilization coefficient from approximately 0.2 to about 0.7. Figures 2, tables 2.

**Influence of Repeated Hardening on Microstructure and Mechanical Properties of ShKh15 Steel**

917D0143A Moscow IZVESTIYA VYSSHIKH  
UCHEBNYKH ZAVEDENIY: CHERNAYA  
METALLURGIYA in Russian Feb 91 pp 48-51

[Article by B. I. Maksumov, I. O. Khazanov, Dushanbe Pedagogic Institute]

UDC 669.018.24-15

[Abstract] The purpose of this work was to optimize heating modes for repeated hardening of ShKh15 bearing steel to reduce the austenite grain size and improve the strength and reliability of rolling bearings in use. Optimal rehardening modes were selected based on the statistical data obtained on the mean grain diameter as a function of temperature variation in repeated hardening. Repeated hardening with first hardening temperature 850°C and second hardening temperature 830°C yielded a fine grain structure with average diameter 4.5-5.1µm. Mechanical properties were improved by 12%, durability was more than tripled, and the reliability of the results of the studies was confirmed. Figures 3; References 5: Russian.

### Chill Casting of High-Strength Cast Iron Body Parts

917D0145B Moscow LITEYNOYE PROIZVODSTVO in Russian Feb 91 pp 24-25

[Article by L. A. Solntsev, V. D. Shifrin, A. S. Nadzhafov, R. D. Dzhabarov, Kharkov Institute of Motor Vehicles and Roads]

UDC 621.74.043.1

[Abstract] The manufacture of body parts of cast steel involves a number of technological and economic difficulties. Manufacture of single-piece castings of cast iron is promising. Preference must be given to chill mold casting by the sandwich process using Fe-Si-Mg master alloy type ZhKMg-1. One-piece castings using type VCh40 material has been used to save 600 tons of rolled steel annually, also reducing the labor consumption of the manufacturing process.

### Status and Prospects for Development of Precision Casting in Lined Chill Mold

917D0145A Moscow LITEYNOYE PROIZVODSTVO in Russian Feb 91 pp 21-23

[Article by V. M. Koshevatskiy, S. B. Kantor, L. M. Kanevskiy, V. I. Mazurik, "NIISL" Scientific-Production Association]

UDC 621.74.043

[Abstract] The authors' association, as well as other enterprises and organizations, has gained experience in the production of complex-shaped castings of ferrous alloys in a lined chill mold, producing such products as motor vehicle camshafts, combine and tractor motor crankshafts, low-carbon steel railroad hitches, cylinder sleeves, electric motor yokes and reducing transmission cases. Automatic production lines have been developed and are in successful use. Future development of the process will apparently involve the creation of universal

automatic production lines and carousel high-productivity units for mass production of precision parts by this method. The authors' association has developed the A133 universal automatic production line with chill molds measuring 1300x1000 mm. The search is on for means to reduce the environmental consequences of the process by the creation of nontoxic clanging mixtures based on inorganic materials and development of systems to neutralize toxic gases evolved in the process. References 2: Russian.

### Reaction of Hydrogen With Ti<sub>4</sub>Fe Alloys

917D0144J Moscow IZVESTIYA AKADEMII NAUK SSSR: SERIYA METALLY in Russian Jan 91 pp 199-201

[Article by V. N. Verbetskiy, R. R. Kayumov, K. N. Semenenko, Moscow]

UDC 669.15'295:661.986

[Abstract] A study is presented of the reaction of Ti<sub>4</sub>Fe with β-Ti structure with hydrogen. At 573-673 K hydrogenolysis occurs forming TiH<sub>2</sub> and TiFe. At room temperature Ti<sub>4</sub>FeH<sub>8.3-8.8</sub> with titanium hydride structure is formed. At high pressures the hydride phase is converted to TiH<sub>2</sub> and iron. A desorption isotherm is obtained for the first time in the system Ti<sub>4</sub>Fe-H<sub>2</sub>. It is found that disproportionation of Ti<sub>4</sub>FeH<sub>x</sub> under high pressure conditions occurs similarly to hydrogenolysis of TiFe when treated with hydrogen under a pressure of up to 100 atm. Figures 2; References 9: 5 Russian, 4 Western.

### X-Ray Measurement of Residual Stresses in Thin TiN Coatings

917D0144I Moscow IZVESTIYA AKADEMII NAUK SSSR: SERIYA METALLY in Russian Jan 91 pp 179-186

[Article by S. Ya. Betsofen, L. M. Petrov, Moscow]

UDC 660.295'786:539.389.3

[Abstract] An attempt is made to interpret the results of measurement of microstresses from the standpoint of the properties of TiN coatings. X-ray studies were performed on specimens of stainless steel, EI961 steel and VT3-1 titanium alloy with coatings of TiN 5-10 µ thick. Compressive stresses as great as 3000 MPa were found. In coatings with poor adhesion an unusual diffraction effect was noted, splitting of reflexes into two lines, due to the difference in residual stresses in grains of the main texture component and in grains with different orientation. The splitting effect corresponds to the case in which  $\sigma_{<111>}$  exceeds the coating failure stress, and the stresses are relaxed by a failure of coating continuity. Figures 4; References 8: 1 Russian, 7 Western.

**Properties of Crystallitons Upon Superplastic Deformation of Fine-Crystalline Materials**

917D0144H Moscow IZVESTIYA AKADEMII NAUK  
SSSR: SERIYA METALLY in Russian Jan 91  
pp 156-160

[Article by V. M. Greshnov, Ufa]

UDC 669.017:539.52

[Abstract] A previous work suggested a phenomenological model for superplastic deformation, consisting of an ideally viscous nutonion fluid with a set of quasiparticle excitations which were called crystallitons. This article presents an experimental study of the basic properties of these crystallitons which define the superplastic deformation of fine crystalline VT9 alloy and Zn+22%Al. The variation of energy, effective mass and velocity of a crystalliton with temperature, material grain size and mechanical system of deformation is established. Physical interpretation of the crystalliton properties established in this work must await theoretical derivation of the basic characteristics as functions of the structural parameters and external conditions of deformation. Figures 2; References 3: Russian.

**Structure and Phase Composition of Contact Zones of Bimetals Produced by Explosive Welding**

917D0144F Moscow IZVESTIYA AKADEMII NAUK  
SSSR: SERIYA METALLY in Russian Jan 91  
pp 138-144

[Article by N. V. Popova, V. Z. Kutsova, A. G. Krimmel, T. N. Rulla, Yu. Ye. Orlenko, A. Yu. Shmelev, Dnepropetrovsk]

UDC 669.017-429:620.18

[Abstract] The contact zone of a bimetallic system consisting of stainless steel and AMg6 alloy obtained by explosive welding was studied to determine the parameters of the wavy boundary with an intermediate layer of technical aluminum. Discontinuities, large inclusions of intermetallic phases in the steel plus technical aluminum contact zone and zones of mechanical motion in the alloy plus technical aluminum contact zone were found. Figures 3; References 2: Russian.

**Phase Composition and Properties of Nickel Casting Alloy With Variable Titanium and Aluminum Content**

917D0144E Moscow IZVESTIYA AKADEMII NAUK  
SSSR: SERIYA METALLY in Russian Jan 91  
pp 129-134

[Article by V. D. Kireyev, N. V. Kolyasnikova, N. T. Travina, Ye. N. Ugarova, V. G. Gontmakher, Moscow]

UDC 669.245.018

[Abstract] A study is made of the influence of titanium, the relationship of titanium to aluminum and the total of titanium and aluminum on the phase composition, structure and properties of complexly alloyed Rene 80 casting alloy hardened by a gamma phase containing 12.6 at.% refractory elements, 16.5 at.% Cr and 0.1 at.% Nb. It is found that the relationship of the content of titanium to aluminum should be 0.7-0.9:1, with total concentration of these elements not over 15.4 at.%. The resultant alloy structure is stable under high-temperature usage conditions. Figures 2.

**Change in Structure of Iron and Steel Upon Very Deep Penetration of High-Velocity Particles**

917D0144D Moscow IZVESTIYA AKADEMII NAUK  
SSSR: SERIYA METALLY in Russian Jan 91  
pp 124-128

[Article by S. M. Usherenko, S. I. Gubenko, V. F. Nozdryn, Dneproetrovsk]

UDC 534.2:621.385.833

[Abstract] The phenomenon of very deep penetration of dispersed high-velocity particles into a metal matrix and the mechanism of its hardening were studied on the example of analysis of the microscopic and fine structure of type EZ steel and armco iron following hot deformation and annealing. The particles were accelerated to 2 km/s, achieving pressures of collision with the target of over 15 GPa. Particle sizes were 40-125 micrometers. The studies showed that the target material experienced significant deformation in the channel zone, leading to softening of the material. Wave effects related to the motion and deceleration of the particles can result in the formation of particle chains along the wave bands of slipping or subboundaries. These chains of inclusions generate stress waves of their own, manifested as the appearance of wave slip lines. The closed nature of these zones indicates complex shear-rotation deformation. Figures 2; References 9: Russian.

**Plastic Deformation of Polycrystalline Beryllium at 400-850 K**

917D0144C Moscow IZVESTIYA AKADEMII NAUK  
SSSR: SERIYA METALLY in Russian Jan 91 pp 88-96

[Article by V. P. Zharinov, A. N. Pavlychev]

UDC 669.017:539.389.2

[Abstract] A study is made of the plastic deformation of hot-pressed beryllium at 400-850 K. Tests were performed on a rigid test machine using flat specimens with a cross section of 1.5 x 2 mm, gage section length 10 mm oriented across the pressing axis. Experiments were performed in air. The Portevin-Le Chatellier effect

causes instability of plastic deformation, with deformation rate in the moving Luders band exceeding the speed of movement of the machine by two or three orders of magnitude at temperatures of less than 700 K. A model is suggested, describing the instability of plastic deformation and the negative speed sensitivity in the area of the Portevin-Le Chatellier effect. Figures 5; References 13: 4 Russian, 9 Western.

### Kinematic Models Considering Nonuniformity of Deformation in Rolling

917D0144B Moscow IZVESTIYA AKADEMII NAUK SSSR: SERIYA METALLY in Russian Jan 91 pp 76-80

[Article by Yu. I. Kamenshchikov, L. A. Barkov, A. Yu. Kamenshchikov]

UDC 621.771.011

[Abstract] A kinematically possible field of velocities of movement of metal particles in the deformation focus during rolling of a rectangular cross section blank in two smooth rolls is studied, considering the nonuniformity of distribution of deformation through the height of the deformation focus. Partial solutions are presented for kinematically possible trajectories of motion, as well as equations to compute the spreading of a strip in the plane of symmetry and on the contact surface. Figure 1; References 4: Russian.

### Thermodynamic Specifics of Steel Refining With Blowing of Silicocalcium Powder

917D0144A Moscow IZVESTIYA AKADEMII NAUK SSSR: SERIYA METALLY in Russian Jan 91 pp 20-24

[Article by A. G. Tyurin, G. G. Mikhaylov]

UDC 669.046.017.3

[Abstract] Estimates are presented of the thermodynamic capability of processes of homogeneous and heterogeneous refining in steel when powders of silicocalcium are blown through the melt. Cross sections of diagrams of homogeneous and heterogeneous refining in metal melts of the system Fe-Mn-Ca-Si-Al-O-S-C. The significance of synthetic slag in the process of desulfuration of the metal under the experimental conditions is determined. It is found that with aluminum concentrations in the steel of 0.001-0.05% as the silicocalcium is blown through equilibrium occurs between the metal and the liquid lime-alumina slag. Secondary oxidation of the steel can at least partially block the process of desulfuration by the synthetic slag. With a carbon content in the steel of up to 1%, calcium carbide is thermodynamically unstable in the metal melt. However, its traces are constantly present when silicocalcium is blown through. If the carbon concentration exceeds 0.16%, calcium carbide can be segregated from the melt in the crystallization zone, and must be carried away into the slag, the ladle lining and oxidized by the atmosphere, or

dissolve once again in the melt after the calcium liquid or vapor phase disappears. Figures 3; References 22: 18 Russian, 4 Western.

### Problems of Heating Furnace Automatic Process Control System Design

917D0143D Moscow IZVESTIYA VYSSHIKH UCHEBNYKH ZAVEDENIY: CHERNAYA METALLURGIYA in Russian Feb 91 pp 93-96

[Article by Ye. V. Toropov, V. I. Panferov, All-Union Scientific Research Institute of Metal Products Industry]

UDC 621.78.04:658.52.011.56

[Abstract] The history of development of control systems for heating furnaces is traced, from manual regulation through simplified automatic regulators to today's modern systems with feedback based on the temperature of the metal. Since it is impossible to measure the temperature of the interior of a piece of metal in a furnace, control must actually be based on a mathematical model relating the internal temperature to the measurable surface temperature. The problem is far from its final solution. Simple, noise-immune (robust) and high-speed identification algorithms are required which consider the relationships between control system, furnace and metal. The heating process must be intensified in the areas of the furnace through which the metal passes last in order to minimize scale formation and power consumption. The algorithmic basis for accurate temperature control considering this need does not yet exist. References 28: Russian.

### Local Morphology of Graphitized Steel Hardened With Induction Heating

917D0143B Moscow IZVESTIYA VYSSHIKH UCHEBNYKH ZAVEDENIY: CHERNAYA METALLURGIYA in Russian Feb 91 pp 53-55

[Article by G. A. Berlin, V. M. Zhurakovskiy, V. S. KhloMOV, Rostov-na-Donu Metal Products Plant]

UDC 669.15-196:543.063

[Abstract] A study is presented of the morphology and mechanism of formation of near-graphite metal base zones in graphitized steel hardened with induction heating. Studies were performed on type 12S2L steel produced by investment casting. Metallographic, x-ray, spectral and durometric analyses were performed. The studies and theoretical analysis of near-graphite areas of the matrix with high microhardness expand the concepts of processes occurring in graphite-containing alloys. This effect can be used to select materials for parts, their structure and phase composition and heat-treatment modes to improve wear resistance and other characteristics. Figures 4; References 6: Russian.

**"(") Conversion in VT30 Titanium Alloy  
Upon Plastic Deformation**

917D0144G Moscow IZVESTIYA AKADEMII NAUK  
SSSR: SERIYA METALLY in Russian Jan 91  
pp 145-148

[Article by M. V. Maltsev, Nizhniy Novgorod]

UDC 669.295:538.214:537.311.31

[Abstract] A study is made of the conversions in titanium alloy type VT30 cooled in water after one hour at

750°C. The quenched specimens were aged at 150-450°C for two hours, considering that the  $\alpha$  phase is segregated at temperatures of not over 450°C. Phase transformations were studied by an x-ray method, indicating a single-phase  $\beta$ -solid solution structure in the specimen quenched from 750°C. Cold plastic deformation caused the martensite conversion  $\beta \rightarrow \alpha'$ . The  $\alpha \rightarrow \alpha'$  (or  $\alpha'$ ) conversion occurs with significant strain hardening. Figures 2; References 8: 3 Russian, 5 Western.

**Stressed State of Carbide Phase of BK6 Hard Alloy During Pulsed Laser Treatment***917D0126J Kiev SVERKHTVERDYIE MATERIALY in Russian No 1, Jan 91 pp 49-56*

[Abstract of article by A. G. Grigoryants, S. I. Yaresko; Kuybyshev branch of the USSR Academy of Science's Institute of Physics]

UDC 621.373.826:621.78:621.9.025.7:548.73

[Abstract] The influence of pulsed laser treatment on the formation of the stressed state of the carbide phase of BK alloys was studied using 4 x 12 x 12-mm multifaceted unsharpened rectangular carbide tips made conventionally from BK6 alloy. Laser treatment was performed on a modernized Kvant-16 laser with pulse energy up to 45 J and pulse duration up to 11 ms at 0.1 maximum power. Energy density was (0.9, 1.1, 1.5, and 1.9)10<sup>6</sup> J/sq m. The treatment process was performed 1, 10, or 100 times per specimen. X-ray phase analysis of the surface layers was performed before and after laser treatment on a DRON-3M diffractometer. Residual stresses in the WC-phase were determined with oblique x-radiography on an RSF-2M Strainflex diffractometer (Rigaku Co., Japan) in Co<sub>Kα</sub>-radiation. The treatment was found to have a selective effect on the stressed state of the carbide phase. After one treatment at energy densities up to 1.5(10<sup>6</sup>), residual tensile stresses steadily increased, and the crystalline lattice acquired a greater degree of imperfection. More intensive changes of the same type took place in specimens subjected to 10 treatments at the same energy densities. Treating the specimens more than 10 times at energy densities greater than 1.5(10<sup>6</sup>) J/sq m was found to be unsuitable, as these conditions destroy the original structure and properties of the carbide phase. A carbide tip can be treated 100 times at the lowest energy density, as this perfects the carbide phase structure. Laser pulse treatment at energy densities up to 1.5(10<sup>6</sup>) J/sq m, with no more than 10 treatments per tip, results in greater tip wear resistance provided they are used within cutting parameters that do not negate the effects of the laser treatment. Figures 4, tables 1; references 10 Russian.

**Effect of Ultradispersed Diamond-Like Carbon Phase Particles on Microstructure of Electrodeposited Chromium Coating***917D0126I Kiev SVERKHTVERDYIE MATERIALY in Russian No 1, Jan 91 pp 46-49*

[Abstract of article by A. L. Vereshchagin, I. I. Zolotukhina, P. M. Brylyakov, V. D. Gubarevich, S. A. Chernykh, N. V. Bychin, V. F. Komarov; Biysk]

UDC 620.22

[Abstract] The properties of a composite electrodeposited chromium-based coating with a diamond-like

carbon phase were studied. The carbon phase is characterized by regions of coherent dispersion 5-10 nm in size and microstresses of up to 10 GPa. The electrolyte had the following composition: 225 g/l of CrO<sub>3</sub>, 0.25 g/l of H<sub>2</sub>SO<sub>4</sub>, 20 g/l of K<sub>2</sub>SiF<sub>6</sub>, and 6 g/l of BaSO<sub>4</sub>. The coating was deposited for 20 minutes at a temperature of 328±2 K and a current density of 50 A/dm<sup>2</sup> onto a copper substrate 0.1 mm thick. Coating thickness was 12-15 μm. The carbon phase, which had a dispersity of 0.05 to 0.2 μm, was deposited in suspension form. Coating microstructure was examined on a DRON-3M diffractometer in molybdenum filtrated radiation and its parameters calculated using the fourth moments technique, starting with an analysis of the chromium reflection profile. Crystalline lattice parameters were calculated from a known value for the center of gravity of the K<sub>α1</sub> line. A model UEM-100B scanning electron microscope was also used to study the coatings. Microhardness was measured on a PMT-3 hardness gauge under a 0.5-1.0 N load. The structure of the surface layers was studied on model VG ESCA-3 (Vacuum Generators Company) and XSAM-800 (Kratos Analytical Company) electron spectrometers. It was found that the carbon phase is introduced into the crystalline lattice of the chromium coating both in the form of a separate phase and while the solid solution and chromium carbide form. For the most part, the particles concentrate in the surface layer of the coating at depths up to 30 nm. As the concentration of the carbon phase in the electrolyte is increased, the size of the coherent dispersion regions decreases, while microhardness increases. Figures 2, tables 3; references: 2 Russian.

**Cold Compacting of CNB Powders at High Pressures***917D0126H Kiev SVERKHTVERDYIE MATERIALY in Russian No 1, Jan 91 pp 41-45*

[Abstract of article by O. N. Andreyev, N. P. Bezhenar; Ukrainian Academy of Sciences Institute of Superhard Materials, Kiev]

UDC 621.762

[Abstract] The effect of compacting pressure and grain size of cubic boron nitride (CBN) powder stock on the porosity, pore size and distribution, and degree of powder comminution in the compacts was studied. KM and KR brand powders with grain size ranging from 1/0 to 80/63 were used. They were charged into a poreless cast copper cylinder and subjected to cold compacting in a high-pressure toroid-type device at P = 1.0-7.7 GPa. Pressure in the compacting chamber was monitored from phase transformations in reference materials. Mercury porometry was used to measure porosity and pore size. Measurements were taken simultaneously from several 1.2-1.5 sq cm specimens produced under identical conditions. It was shown that the classic equations of powder metallurgy describe the relationship between

compacting conditions and compact properties. In particular, porosity as a function of compacting pressure and powder stock grain size is described by an exponential equation. By measuring the resistivity of the powder, the authors were able to determine that larger powder grain size was associated with a higher rate of powder comminution. To measure resistivity, an original technique was used that involved coating the powders with a fine layer of graphite and then compacting them in the same manner as the powders not coated with graphite. Resistivity was measured directly during compacting by a Shch-34 probe built into the die assembly. The graphite coating does not have an appreciable effect on compact properties, so the graphite-coated powders serve as a useful proxy for measuring the properties of uncoated powders. In addition to the comminution rate, CNB grain size has a substantial effect on the initial comminution pressure. Figures 4; references 11: Russian.

#### **Effect of Surface Chemical Composition of Synthetic Diamond Micropowders on Polycrystals Sintered From Them**

917D0126G Kiev *SVERKHTVERDYIE MATERIALY* in Russian No 1, Jan 91 pp 37-41

[Abstract of article by V. G. Aleshin, A. A. Smekhnov, M. G. Chudinov, V. A. Shishkin, A. A. Shulzhenko; Ukrainian Academy of Sciences Institute of Superhard Materials]

UDC 539.134

[Abstract] Synthetic diamond micropowders and polycrystals made from these powders were studied to determine how the properties of the crystals are affected by the surface chemical composition of the powders. The specimens were first examined using x-ray photoelectron spectroscopy, Auger electron spectroscopy, and secondary-ion mass spectrometry. ASM 7/5 diamond powders were then chemically treated by boiling them in hydrochloric acid for one hour, then rinsing them several times in distilled water. This was followed by vacuum annealing at 1325±25 K and approximately  $10^{-2}$  Pa. The specimens were then reexamined. It was found that chemical treatment reduces the total impurity content of the powders. Impurities reduced include nitrogen, oxygen, silicon, boron, calcium, magnesium, and iron. The purest powders were obtained by vacuum annealing at high temperatures. Chemical pretreatment and annealing also substantially reduced the level of surface impurities in particles obtained by fracturing polycrystals sintered from powders with grain sizes ranging from 5/3-7/5 to 60/40. The mechanical properties—hardness, strength, and wear—and resistivity of sintered polycrystals were also tested and were found to improve when the polycrystals were sintered from chemically pre-treated and annealed powders. Figures 3, tables 3; references 7: 6 Russian, 1 Western.

#### **Hardness and Cracking Resistance of Materials Based on Dense BN Modifications**

917D0126F Kiev *SVERKHTVERDYIE MATERIALY* in Russian No 1, Jan 91 pp 34-36

[Abstract of article by S. N. Dub, A. I. Ignatusha; Ukrainian Academy of Sciences Institute of Superhard Materials]

UDC [621.921.3:661.65]:539.533

[Abstract] The hardness and cracking resistance of a number of materials based on dense modifications of boron nitride were measured. The single-layer materials tested were: kyborite, amborite (Great Britain), 05 IT composite, RKVN-15 (Czechoslovakia), and composite 10. Double layer materials were: BPK, composite 02, BZN compact (United States), 05 IT composite, RKVN-A15, sumiboron BN 200 (Japan), composite 10 D, and nyborite. Hardness was measured with a Knoop indenter under a load of 4.91 N on a PMT-3 microhardness gauge. Cracking resistance was measured by finding the length of cracks radiating from indentations made by Vickers and Berkovich indentors on a model TP-2 Vickers hardness gauge. Indentation size and crack length were measured with the aid of an NU-ZE microscope. Kiborite and BPK had the highest values for cracking resistance in combination with hardness. Figures 1, tables 1; references 5: 4 Russian, 1 Western.

#### **High-Temperature Strength of Polycrystalline Boron Nitride With Titanium Nitride-Based Binder**

917D0126E Kiev *SVERKHTVERDYIE MATERIALY* in Russian No 1, Jan 91 pp 27-30

[Abstract of article by I. M. Androsoy, V. T. Vesna, V. P. Maslov, Ukrainian Academy of Sciences Institute of Superhard Materials; V. A. Ponomarenko, Ilyich Abrasives Plant, Leningrad]

UDC 621.762

[Abstract] The strength and cracking resistance of composite 06, a new polycrystalline superhard material, and of 05-IT as a function of temperature were studied. Both materials consist of polycrystalline boron nitride with titanium nitride binder concentrations of 10, 25, and 30%. The specimens were disks 7 mm in diameter and 1 mm thick. The tests were performed in a vacuum (up to  $10^{-2}$ ) on a modernized IMASh 20-75 testing machine equipped with a special high-temperature combination load application device and reversing mechanism. Testing temperatures ranged from 300 to 1400 K. A P2 platinum and platinum-rhodium thermocouple was used to measure temperature directly on the specimen surfaces. The rate of deformation did not exceed 1.6 mm/minute. The specimens were subjected to center-line compression. To test for cracking resistance, electroerosion was used to put a crack-simulating notch through



the center of the specimens, and load direction coincided with the notch line. In specimens with a 30% or 25% binder content, strength gradually decreased from room temperature to 1000 K, above which the decrease was more pronounced. Between 1100-1300 K, strength increased somewhat. Strength in specimens with 10% binder was virtually unaffected by temperature. Cracking resistance was constant between 300-1100 K, above which it declined substantially. It was recommended that cutting tools made from composites 06 and 05-IT with 30% binder not be used at temperatures exceeding 1100 K and that new boron nitride materials be developed by modifying the binder components and concentrations. Figures 2; references 6: Russian.

### Studying the Stressed State of Elboron-P Polycrystals

917D0126D Kiev *SVERKHTVERDYE MATERIALY* in Russian No 1, Jan 91 pp 25-27

[Abstract of article by V. A. Pesin, Ya. I. Kunin, V. I. Monin, T. M. Svyazkina; VNIASH NPO, Leningrad]

UDC 539.319:621.922

[Abstract] X-ray diffractometry was used to study the stress-strain state of elboron-P polycrystals (matrix sphalerite phase -  $\text{BN}_{\text{sp}}$ ) with different concentrations (0 to 12%) of residual graphitic BN ( $\text{BN}_g$ ) before and after heat treatment. Residual stresses were determined from oblique x- radiographs taken by a DRON-UM1 diffractometer using an RKD-1 coordinate detector along elboron line 331 in  $\text{CuK}_\alpha$ - radiation. Microstresses associated with broadening were located along lines 220 and 331 using Koshi approximation. Stresses in the  $\text{BN}_g$  phase were measured by shifting the center of gravity of  $\text{BN}_g$  line 002. Diffraction lines  $\text{BN}_{\text{sp}}$  220 and 331 and  $\text{BN}_g$  002 were recorded on a DRON-2 diffractometer in discrete mode with  $0.05^\circ$  increments in  $\text{CuK}_\alpha$ -radiation. All computations were done on an Iskra-1256 computer. The specimens were heat treated in air at 400, 600, 800, and  $1000^\circ\text{C}$  with a holding time of 15 minutes, after which they were air-cooled. Graphite content, which was determined from the intensity of the  $\text{BN}_g$  line, was not affected by heat treatment. In their initial state, cylindrical elboron specimens had tensile stresses in the facial surfaces. Without residual  $\text{BN}_g$ ,  $\sigma$  was 0.10-0.15 GPa; with residual  $\text{BN}_g$ , it was 0.20-0.40, with a tendency to increase as  $\text{BN}_g$  content increased. The residual  $\text{BN}_g$  was highly compressed (1.5-2.1 GPa). Partial relaxation of stresses occurred during heat treatment as a result of microfissuring of the  $\text{BN}_{\text{sp}}$  matrix near the  $\text{BN}_g$  inclusions. Elboron-P with residual  $\text{BN}_g$  was found to be very sensitive to heating. Residual  $\text{BN}_g$  plays a decisive role in the formation of the stressed state of elboron-P and in the relaxation of these stresses during heat treating. Figures 2, tables 1; references 5: Russian.

### Change in the Impurity Composition of Synthetic Diamond Single Crystals During P-T Treatment

917D0126C Kiev *SVERKHTVERDYE MATERIALY* in Russian No 1, Jan 91 pp 14-17

[Abstract of article by V. G. Malogolovets, G. V. Chipenko, S. A. Ivakhnenko; Institute of Superhard Materials of the Ukrainian Academy of Sciences, Kiev]

UDC 535.33:666.233

[Abstract] IR spectroscopy was used to study the effects of P-T treatment on impurity centers in synthetic diamonds. The study was carried out using a UR-20 spectrophotometer with its own microattachments. Specimens studied were a crystal serving as the control, produced from an Ni-Mn-C system, no visible inclusions, with well-defined faces, and containing C-center nitrogen impurity only; two crystals of IIv-type semiconductive diamonds, one produced from an Ni-Mn-C system using Ti as the nitrogen getter, the other produced from an Mg-Zn-C system; three crystals synthesized in an Ni-Mn-C system and containing D-dendrites in addition to paramagnetic nitrogen; and three crystals displaying in the spectra intensive absorption at wave numbers of 820, 870, 920, and  $960\text{ cm}^{-1}$ . P-T treatment was carried out in a toroidal high-pressure apparatus, using spectrally pure graphite as the annealing medium. Annealing temperature was kept within  $+50\text{ K}$ . The IR spectra for the Mg-Zn-C and Ni-Mn-C-Ti diamonds revealed that, during P-T treatment, the nitrogen impurity atoms migrate around the crystal. These atoms are captured by boron impurity atoms, leading to the formation of non-paramagnetic D-centers. The P-T process did not have much of an effect on the content of D-centers in those specimens that contained them. However, in those specimens with Me-X impurity centers, P-T treatment resulted in noticeable changes in the single-background component of the absorption spectrum. The presence of D and Me-X centers in the crystals influences the extent to which paramagnetic nitrogen impurity can be transformed into A-centers during P-T treatment. The D-centers are resistant to the effects of this process and reduce the extent of nitrogen aggregation. The Me-X centers break down, with the freed nitrogen going to form the A-centers. Figures 2; references 12: 6 Russian, 6 Western.

### Effect of Trap Energy Structure on Injection Properties of Contacts on a Synthetic Diamond

917D0126B Kiev *SVERKHTVERDYE MATERIALY* in Russian No 1, Jan 91 pp 6-10

[Abstract of article by L. A. Romanko, A. G. Gontar; Institute of Superhard Materials of the Ukrainian Academy of Sciences]

UDC 621.315.592

[Abstract] Space charge-limited currents were used to study how the type, number, and spectral distribution of

electrically active flaws in high-ohm synthetic diamonds affects the charge carrier injection properties of titanium contacts affixed to these diamonds. Specimens were made from type Ib high-ohm diamond single crystals. Some of the crystals were pre-annealed at 1400°C. The specimens were typically up to 0.5 sq mm in area and from 0.09 to 0.25 mm thick. Electrical contacts were affixed to them by vapor deposition of titanium in a  $1.3(10^{-3})$  Pa vacuum. Volt-ampere characteristics were measured in a cryostat in a vacuum with a residual gas pressure of 0.013 Pa at temperatures of 25, 50, and 100°C. Current was measured by V7-29 and V7-30 electrometers at noise levels of  $10^{-17}$  and  $10^{-15}$ , respectively. Each VAC was recorded when current reached a preset value after voltage application. The transfer of charge carriers inside the specimen was found to depend to a great extent on the characteristics of the contact zone, which are determined by the processes involved in the formation of the metal film and by the energy structure and concentration of energy levels in the forbidden band of the diamond. High-temperature annealing did not affect the energy structure of the traps and thus did not play a role in how the space charge affected the contact properties. Complete or partial compensation for the space charge of the deep traps is possible if low-energy traps ( $E_a = 0.26-0.40$  eV) capture carriers with the opposite sign. Since it is rather difficult to use external means such as ionizing radiation to create energy levels with the required properties in synthetic diamonds, it is necessary to select specimens with the required energy level spectrum in the forbidden zone in order to produce contacts with the required properties. Figures 4; references 3: 2 Russian, 1 Western.

#### **Autoradiographic Study of Diamond Crystals and Carbide Phases**

917D0126A Kiev SVERKHTVERDYIE MATERIALY  
in Russian No 1, Jan 91 pp 3-5

[Abstract of article by A. A. Putyatin, V. I. Korobkov, O. V. Madarova; Moscow]

UDC 666.233

[Abstract] Individual diamond crystals and carbide phases were autoradiographically studied to further clarify the role carbides play at various stages of Me-C diamond formation. The radiographs were obtained by calculating the duration of specimen exposure on type-R radiophotographic plates, which ranged from 2 to 8 hours, from specific carbon radioactivity in the diamonds and carbides. The diamond surfaces, carbide sections, and autoradiographs were studied on MBS-1, MBR-1, and MBB-1A optical microscopes. The range of magnification was 10-80. The diamond crystals were also studied on an Hitachi F 800 scanning electron microscope within a magnification range of 150-400. The results corroborated previous conclusions stating that two carbon sources, graphite and carbide, contribute to the nucleation and growth of the diamond

phase. Depending on growth conditions, one source may predominate in the crystallization process. The carbide carbon uniformly completes the final structure of the surfaces of perfect crystal faces. It can be presumed that, the greater the contribution of this carbon to the final structure of the crystal face, the more perfect the face. Figures 3; references 6: Russian.

#### **Use of Ultrafine-Grain Aluminum Alloys in Crucial Design Parts**

917D0127G Moscow TSVETNYIE METALLY  
in Russian No 12, Dec 90 pp 87-91

[Article by M.Kh. Rabinovich and M.V. Markushev, UFAI (Ural Division of Aluminum Institute) imeni S. Ordzhonikidze]

UDC 669.715:624.014.7

[Abstract] A study of the effect of grain size of aluminum alloys on their resistance to crack nucleation and growth under quasi-static, impact, and fatigue loading is reported. It was found that grain refinement, including ultra-refinement, increases the crack growth rate and inhibits crack nucleation regardless of the mode of loading, but the relationship between the resistance to crack nucleation and the resistance to crack growth changes with the nature of the material and the mode of loading. Therefore ultrafine-grain materials should be selected when their service life can be limited to the time necessary for crack nucleation under a given load and when their lower resistance to crack growth can be tolerated for a determined time. Figures 3; tables 3; references 18: 12 Russian, 5 Western, 1 Japanese.

#### **Effect of Annealing Practice on the Properties of Copper-Clad Aluminum Wire**

917D0127A Moscow TSVETNYIE METALLY  
in Russian No 12, Dec 90 pp 81-83

[Article by B.M. Zhukov and V.I. Romanovskiy, VNIKP (All-Union Scientific-Research, Design, and Technology Institute of the Cable Industry) Scientific-Production Association]

UDC 621.74:669.715

[Abstract] Annealing experiments leading to optimization of mechanical properties and electrical resistivity of copper-clad aluminum wire are reported. Clad wire specimens ranging in diameter from 0.8 to 4.41 mm were annealed at 350 to 550 °C for 0.6 to 2.5 hours and tested for bending fatigue resistance, elongation in tensile tests, tensile strength, and electrical resistivity. Maximum elongation and fatigue resistance were observed in specimens annealed at 450 °C. The annealing time at this temperature has little effect on these properties. Elongation at fracture was found to increase considerably with annealing time at 350 °C. Tensile strength was found to decrease with increasing annealing temperature up to

450 °C and with annealing time. Annealing temperatures above 450 °C lead to increased thickness of the intermetallic zone between aluminum and copper and consequently to increased strength. Electrical resistivity decreases with increasing annealing temperature up to about 350 °C and increases sharply at higher temperatures. The results are explained in terms of the composition and thickness of the intermetallic zone. Best combination of properties is obtained by annealing for 0.5 to 1.5 hours at 350 to 400 °C. Five figures; two Russian references.

**Problems of Establishment of Small Specialized Enterprises in the Industry Engaged in Working and Processing of Nonferrous Metals and Alloys**

917D0127E Moscow TSVETNYE METALLY  
in Russian No 12, Dec 90 pp 76-78

[Article by G.N. Strakhov, GIPROTSVETMETOBRABOTKA (State Scientific-Research and Design Institute for Alloys and Treatment of Nonferrous Metals)]

UDC 621.7:669.2

[Abstract] Until recently it was considered that modernization of existing production facilities and construction of new facilities at old plants was the most economical and efficient way of increasing the industrial production. In the nonferrous metalworking industry modernization has failed to create modern plants and increase the production to the desired levels. It is now thought that establishment of small specialized private, cooperative, or stock enterprises, which has been made possible by recently enacted laws, is a better alternative to modernization of old facilities, especially because of the transition to market economy. The author lists a number of suggestions of products and processes developed in the Soviet Union that are suitable for small specialized enterprises in the nonferrous metalworking industry. The suggestions cover the production of tubular products, wire rod and wire, and strip.

**Defect Formation During Growth of Silicon Multilayer Epitaxial Composites**

917D0127D Moscow TSVETNYE METALLY  
in Russian No 12, Dec 90 pp 74-76

[Article by P.N. Galkin, O.P. Golovko, V.P. Tokarev, V.Ye. Bakhrushin, and A.I. Rozhkov, ZTMK (Zaporozhye Titanium-Magnesium Combine) and Zaporozhye Industrial Institute]

UDC 621.315.592

[Abstract] A metallographic study of shear lines and lattice defects associated with them in p-n-n<sup>+</sup> and n<sup>+</sup>-n<sup>+</sup> silicon composites with multiple epitaxial films alloyed with phosphorus and boron is reported. One type of shear lines starts at microcracks at the edge of silicon

platelets, spreads toward the platelet center along the <110> direction, and penetrates the substrate and both epitaxial layers. In the substrate the shear lines consist of one or more parallel rows of dislocations in which the dislocation lines are inclined at the same angle to the surface being observed. In the epitaxial films the shear lines contain dislocation loops, stacking faults, and Frank's dislocations. This pattern arises because the shear step that forms as a result of formation of a row of dislocations in the substrate at the start of epitaxial film growth is a source of stacking faults and dislocation loops in the film. The other type of shear lines go only through the epitaxial films and are due to a step that forms as a result of local disturbances in the structure of the substrate surface, such as small scratches or local deformations of the crystal lattice. The structure of the lower epitaxial film was found to be much less perfect than that of the upper film. Networks of mismatch dislocations with dislocation densities between 1000 and 10,000 per square cm were found at the interfilm boundary when the upper film was alloyed with boron and the lower film with phosphorus, but not when both films were alloyed with phosphorus. Dislocation networks were also found when phosphorus-alloyed films were deposited on an antimony-alloyed substrate, but not when the substrate and the films were alloyed with phosphorus. It was found that stacking faults do not spread from the lower film to the upper film if the platelets are transferred to another reactor prior to the deposition of the second film; that is, when the first film is exposed to the atmosphere prior to the deposition of the first film. It is concluded that the probability of formation of shear lines can be reduced if crack formation at the substrate periphery is prevented by proper machining. Two figures; two Russian references.

**Factors Affecting the Quality of Protective Coatings on Magnesium**

917D0127C Moscow TSVETNYE METALLY  
in Russian No 12, Dec 90 pp 30-36

[Article by A.Ye. Stolina and V.I. Gribov, Berezniki Division of the Titanium Institute]

UDC 669.721.8

[Abstract] The effect of chloride concentration in 3 g/l potassium dichromate chromating solution, of dichromate concentration in chromating solution, of chromating temperature, and of cleaning of magnesium surface before chromating on corrosion resistance of magnesium and its alloys in 0.1 percent NaCl solution is reported. Chloride concentrations up to 0.4 g/l in 3 g/l dichromate solution have no effect on corrosion of magnesium. A large corrosion rate increase occurs at chloride concentration of 0.8 g/l in the chromating solution; this is attributed to the lack of integrity of the chromate coating produced at this chloride concentration. Corrosion rate was found to fall by a factor of 10 in the case of magnesium and by a factor of 100 in the case

of magnesium alloy MA8TsCh as the potassium dichromate concentration in the chromating solution increases from 1 g/l to 10 g/l; this is attributed to increased coating density with increasing concentration of potassium dichromate. An increase of chromating temperature from 20 to 80 °C has little effect on corrosion rate of magnesium MG90 and magnesium alloy MA8TsCh but increases the corrosion rate of magnesium MG95 by a factor of four. Cleaning of magnesium surface in soda solution followed by rinsing in water was found to increase the corrosion resistance of magnesium and of magnesium alloy MA8TsCh by improving the bonding between the substrate and the chromate coating. Figures 4; tables 3; 3 Russian references.

**Development of Automation Systems for Lead and Zinc Production Processes on the Basis of Noise-Proof Algorithms**

917D0127B Moscow TSVETNYYE METALLY  
in Russian No 12, Dec 90 pp 36-38

[Article by Yu.M. Abdeyev, V.V. Terekhin, and G.K. Shadrin]

UDC 669.431-52

[Abstract] A method of synthesis of noise-proof control algorithms and their use in the lead-zinc industry is reported. The synthesis involves compensation of disturbances with the use of inverse models of the units that are to be controlled and inclusion of a standard filter in the compensation circuit. The method is illustrated by synthesis of control algorithms for a linear multidimensional system. A nonlinear inverse model that compensates nonlinearity can be constructed for a nonlinear unit. The method was successfully used in the lead-zinc industry for setting up of PI-controllers, control of electric power, automatic maintenance of constant charge-to-oxygen and charge-to-clinker ratio in the KIVTsET lead-production process, control of furnace temperature for roasting of zinc concentrates, control of pH in production of lead salts, and development of an automated metering system for particulate bulk materials. Two figures; three Russian references.

**Autogenous Lead Production Method in the KIVTsET-TsS Unit**

917D0127A Moscow TSVETNYYE METALLY  
in Russian No 12, Dec 90 pp 30-36

[Article by A.P. Sychev, I.P. Polyakov, Yu.A. Grinin, and Yu.I. Sannikov]

UDC 669.431

[Abstract] The present state of the KIVTsET-TsS process (oxygen-flash-smelting cyclone-electrothermic zinc-lead process) for lead production from lead and lead-zinc concentrates in the Soviet Union is reported. A listing of completed research projects leading to the present state

is followed by description of two planned and one completed lead production facilities. The research projects include the process kinetics and selective reduction of lead, heat and mass transfer during reduction in the coke filter, analytical description of flash smelting, conditions of autogenous flash smelting of sulfide concentrates together with oxidized concentrates, separation of lead from zinc, the use of coal and Waelz slag instead of coke breeze, removal of copper from lead bullion, optimization of dimensions of individual zones of the KIVTsET unit leading to reduction of consumption of heat from external sources, stabilization of reduction in the coke filter when the flash-smelting parameters vary, and identification of pollution sources of the process and pollution abatement. The existing lead smelter at the Dalpolimetall Production Association Lead Plant in Rudnaya Pristan on the shore of the Sea of Japan is to be converted to the KIVTsET process, which will quadruple the present production capacity. The new plant will smelt Far-Eastern lead concentrates containing 65% Pb and 5% Zn together with silver-bearing Dukat concentrates. Its products will be commercial lead, sulfuric acid, zinc vitriol, precious-metal alloy, metallic bismuth, and granulated slag for use as concrete aggregate for back-filling of mine cavities. The existing KIVTsET smelter at the lead plant of the Ust-Kamenogorsk Lead-Zinc Combine will be upgraded, and its capacity will be increased to 750 tpd of charge materials. The smelter will process lead-zinc sulfide concentrates containing 52.3% Pb and 7.5% Zn, lead filter cakes containing 33.7% Pb and 8% Zn, and purchased lead-bearing dusts containing 42% Pb and 12.2% Zn. Waelz slag will be used as reducing agent instead of coke breeze. The modernized plant will produce commercial lead, copper matte, lead-zinc slag sublimates, cadmium-rich electrostatic-precipitator dust, precious-metal alloy, sulfuric acid, and byproducts containing bismuth, antimony, and tellurium. The modernization will cost 208 million rubles. At the Chimkent Lead Plant the lead production process consisting of smelting of agglomerated charge in shaft furnaces will be replaced by the KF-KF (oxygen-flame-coke-filter) version of the KIVTsET process. Blending of charge materials by stacking and reclaiming will be replaced by blending in water followed by filtering and drying. The process features very low consumption of electric power (30 to 40 kWh per ton of charge materials). The plant will produce refined lead, lead-zinc sublimates from fuming furnaces, copper matte, sulfuric acid, precious-metal alloy, metallic bismuth, and rare metals. The modernization will cost 68 million rubles. The KIVTsET process is patented in 15 countries. A 600 tpd KIVTsET plant has been built in Italy. One table; 12 references: 11 Russian, one Western.

**Structure and Properties of Aluminum-Copper Welded Joints**

917D0115E Moscow METALLOVEDENIYE I  
TERMICHESKAYA OBRABOTKA METALLOV  
in Russian No 12, Dec 90 p 34

[Article by T.M. Mozhanskaya and N.T. Chekanova, Higher Technical Research Institute attached to ZIL

(Moscow Automobile Plant imeni I.A. Likhachev) and  
ZIL Production Association]

UDC 620.18:669.7153:621.791

[Abstract] Butt welds of aluminum AD1 and copper M2 tubes (8 mm diameter, 1.5 mm wall thickness) prepared by fusion and friction welding are described. The transition zone is 20-25 microns wide (microhardness 82 H) in the case of fusion welding and 10-14 microns wide (microhardness 68 H) in the case of friction welding, which indicates the absence of brittle  $\tau$ -phase primary grains in the transition zone. Formation of aluminum-copper eutectics in fusion welds is indicated by their microhardness and confirmed by scanning microscopy. The transition zone of fusion welds also contains  $\tau$ -phase and a hypereutectic solid solution containing 9.3 at.% Cu and 89.8 At.% Al. Friction welds contain a solid solution containing 2.2% Cu and 96.7% Al and a small quantity of secondary  $\tau$ -Phase. Specimens failed in tensile tests in the aluminum part, which indicates the absence of brittle  $\tau$ -phase in the transition zone. One figure (page facing page 17); one Russian reference.

#### Heat Treatment of Aluminum Bronzes Exhibiting Shape-Memory Effect

917D0115F Moscow METALLOVEDENIYE I  
TERMICHESKAYA OBRABOTKA METALLOV  
in Russian No 12, Dec 90 pp 37-40

[Article by M.A. Kravchenko, V.K. Larin, and S.G. Radchenko, Kiev Polytechnic Institute]

UDC 669.017:621.78:669.018.6

[Abstract] The effects of the ingot solidification rate, the annealing temperature and time, the duration of heating to quenching temperature, the quenching temperature, and the quenching medium on the structure and thermomechanical properties of three bronzes containing 2.7% Mn and 9.4% Al, 6% Mn and 12% Al, and 10.3% Mn and 13.75% Al were studied in order to optimize their heat-treatment aimed at obtaining the best combinations of thermomechanical properties for different compositions. Mathematical models were obtained that are capable of determining the heat treatment practices that maximizes the shape-memory effect of Mn-Al bronzes. It was found that a one-step heat treatment consisting of water-quenching of the bronzes from a temperature at which the  $\beta$ -phase is stable (usually 1175 °K) is insufficient to fully utilize the potential of bronzes as materials exhibiting the shape-memory effect; this requires heat treatment consisting of a high-temperature anneal and air cooling prior to quenching. Optimum heat treatment results in formation of  $\text{Cu}_2\text{MnAl}$  intermetallic compound that increases the parameters of the shape-memory effect. Cu-Mn-Al alloys are recommended as replacement for Ni- and Ti-based alloys exhibiting the shape-memory effect. Figures 2; tables 3; references 3, two Russian, one Japanese.

**Mechanism of Optical Glass Polishing by  
"Akvapol" Tool**

917D0123B Kiev *SVERKHTVERDYIE MATERIALY*  
in Russian No 6, 1990 pp 62-66

[Article by V. V. Rogov, Institute of Superhard Materials, Ukrainian Academy of Sciences]

UDC 681.4.022.2

[Abstract] A study is made of the mechanism of polishing optical glass by a tool with bound powder based on  $\text{CeO}_2$ . It is concluded that the mechanism involves processes of dispersing the glass particles at the molecular level by adhesion or fatigue wear, chemisorption mass transfer of the silicon of the glass by powder grains, hydrolysis of soluble silicates and friction-chemical interactions with the glass and water by salts containing the ammonium cation contained in the polishing composition. The polishing process is intensified by the attachment of the powder by the tool binder, by introduction of chemical activators, and also by the heat generated by friction. Figure 1; References 13: Russian

**Paranite-New Material for Solid-Phase  
High-Pressure Equipment Containers and Seals**

917D0123A Kiev *SVERKHTVERDYIE MATERIALY*  
in Russian No 6, 1990 pp 3-7

[Article by Z. Raab, K. Volshtet, N. V. Novikov, A. V. Gerasimovich, V. G. Malogolovets, N. M. Grigorev, Scientific Research Center of High Pressure, East Germany Academy of Sciences; Institute of Superhard Materials, Ukrainian Academy of Sciences]

UDC 539.893

[Abstract] Paranite is a promising material for use in high-pressure equipment. The authors used Bridgman anvils to test three varieties of paranite specimens. The results of the tests indicate that a multicomponent system of mineral raw material may be preferable to a single-component system when minerals are used as high-pressure equipment containers. By changing the composition of the operating mixture it is possible to change the physical and mechanical properties smoothly, thus adapting them to the specific task at hand. Figures 3; References 4: 3 Russian, 1 Western.

**Technology for Producing a Heat-Resistant Alloy***917D0125H Moscow LITEYNOYE PROIZVODSTVO in Russian No 12, Dec 90 p 23*

[Abstract of article by V. A. Brovkov, A. I. Smirnov, A. I. Brovkova; Karadansk Metallurgical Combine; Temirtauskiy Mechanical Repair Plant]

UDC 621.74.002.6:669.14

[Abstract] A technology has been developed for producing 60KhVYuT high-chromium heat-resistant alloy used to cast riders. The alloy is made in high-capacity IST-04 induction or 1.5-t arc furnaces by fusing FKh025 ferrochromium and then adding ferrotungsten and ferrotitanium 15 minutes prior to tapping, and granulated aluminum. The alloy is also made by charging the ferrochromium and a quantity of ferrotitanium equal to 10% of the ferrochromium charge into the furnace at the same time, then proceeding as before. Slag is not used in either method. Tapping temperature is 1720 to 1740°C; casting temperature 1680 to 1700°C. The second way of making the alloy yields the required chemical composition of greater than 60% chromium and reduces ferrochromium heat loss by 2 to 4%. The chemical composition of the alloy, averaged from 12 melts, was: 0.15% C, 0.9% Si, 61% Cr, 5% W, 0.7% Al, 0.4% Ti, 0.012% S, 0.018% P. The rider molds were dry-formed on Model 233 mold-making machines from a mold mixture with a dry strength greater than 300 kPa. Two coats of zinc paint were applied before and after curing. Retrofitting a 1700 continuous furnace with these riders helped to eliminate uneven slab heating, conserve fuel, and improve hot-rolled sheet quality. References 1: Russian.

**Antimony-Based Alloys for Composite Materials***917D0125G Moscow LITEYNOYE PROIZVODSTVO in Russian No 12, Dec 90 p 22*

[Abstract of article by Yu. I. Rubenchik, I. A. Solovyev, V. A. Gulevskiy, I. D. Busalaye]v]

UDC 621.74:669.755.018.2

[Abstract] Three alloys based on SuO-type antimony (Sb-Sn, Sb-Al, and Sb-Cu) were developed as possible matrix materials for making graphite/metal composites, in which a graphite shell is impregnated with molten metal. The alloys were tested for volatility, shrinkage, penetrating ability, and corrosion resistance. Linear shrinkage was tested on specimens 72 mm long at 700°C. Penetrating ability was tested by measuring the depth to which the molten alloy flowed into from one to three capillary pores (0.45 mm in diameter) made in the bottom of closed flat-bottomed openings 10+1 mm in diameter and 5+1 mm deep formed in the graphite shell. The alloy was isothermally soaked in the opening at 750°C for 20 minutes. Volatility was measured from the relative change in specimen mass after isothermal

soaking for 20 minutes in a weak argon stream. Corrosion resistance was measured gravimetrically. The specimens were made by vacuum suction of the melt into quartz tubes, where it crystallized. The specimens were cut into bars 4 cm in diameter and about 12 cm long, and their end faces were ground and polished. Roughness was  $R_a = 0.16$  to  $0.08 \mu$ . Various aqueous solutions were used as corrosive media. Five specimens were tested in each solution for 20 minutes at 20°C. The results showed that, of the three alloys tested, Sb-Sn alloy had the smallest shrinkage percentage ( $\epsilon = 0.32$  to  $0.334\%$ ), the greatest penetrating ability (1.6 mm), virtually no volatility up to 750°C, and the greatest corrosion resistance. References 1: Russian.

**Influence of Silicon on Properties of Nearly Eutectic Iron***917D0125F Moscow LITEYNOYE PROIZVODSTVO in Russian No 12, Dec 90 pp 21-22*

[Abstract of article by L. S. Volkovicher, B. E. Kletskin; Chelyabinsk Polytechnical Institute]

UDC 621.74:669.131.622

[Abstract] Grey iron was smelted from a charge of P2 conversion pig, 17A scrap iron, ferromanganese, and ferrosilicon in a cupola furnace lined with fireclay. To maintain the accuracy of the chemical composition, none of the product itself was recycled as part of the charge. Each successive charge of metal was separated by a charge of coke, while the eutectics of the experimental irons were kept as close as possible. The temperature of the iron was measured with a VR 5/20 immersion thermocouple. Strength, hardness, chill, and castability tests showed that a lower silicon content resulted in a marked improvement in mechanical properties and castability due to an increase in the quantity of pearlite and a decrease in the quantity of free graphite. There was also an increase in chill depth, which adversely affects the workability of the cast iron. The sensitivity of the iron to the cooling rate was also reduced by decreasing its silicon content. Tables 1.

**Making Fusion-Cast Channels for MDN-6A Magnetohydrodynamic Metering Devices***917D0125E Moscow LITEYNOYE PROIZVODSTVO in Russian No 12, Dec 90 pp 12-13*

[Abstract of article by V. N. Moiseyenko, O. M. Drobot, V. Z. Aronov; Institute of Fusion Casting of the Ukrainian Academy of Sciences]

UDC 621.746.5:66.028

[Abstract] Fusion-cast channels for metering aluminum and zinc alloys on an MDN-6A magnetohydrodynamic metering device are made by fusing a charge made up of

quartz sand, magnesite, alumina, and potassium fluosilicate in proportions that yield potassium fluorophlogopite in the mica crystalline material. Optimally structured mica has a fluophlogopite crystal size of from 1 to 3 mm. The melt is produced in an IST-0.16 induction furnace. Melt temperature is from 1550 to 1600°C. The melt is tapped into a teeming ladle, from whence it is teamed into molds. The molds are made from a single molding compound, air-dried for 24 hours, and then dried by a portable burner prior to assembly. Casting is done for 8 to 10 minutes, after which the molds are opened, and the castings removed and partially cleaned of mold grit. The castings are annealed in a gas-fired reverberatory furnace, soaked for 1 to 2 hours at 900 plus or minus 50°C, and cooled along with the furnace. The fusion-cast channels proved to be highly resistant to the erosion and corrosion associated with aluminum and zinc melts and helped to increase the productivity, versatility, and service life of the foundry equipment in which they were used. Figures 2; references 3: Russian.

#### **Automatic Metering Control in an Electric Furnace Equipped With a Submersible Magneto-hydrodynamic Pump**

917D0125D Moscow LITEYNOYE PROIZVODSTVO  
in Russian No 12, Dec 90 pp 11-12

[Abstract of article by Yu. A. Krylov, V. I. Ruskol, and S. K. Filatov; All-Union Scientific Research Institute of Electrothermal Equipment]

UDC 621.746:669.36

[Abstract] A system for controlling the dispensation of metered amounts of aluminum alloy from electric holding furnaces was described, using a crucible-type furnace equipped with a submersible magneto-hydrodynamic pump as an example. The system was designed to overcome the basic problem of measuring the level of melt in the furnace crucible. The submersible part of the pump is installed in the crucible and consists of a disk chamber with a passageway for the metal and a central intake opening. This chamber is made in one piece from heat-resistance concrete. Beneath the crucible, an electromagnet is installed coaxially with the chamber to create an axial magnetic field. The operating current is supplied by electrodes. Pressure in the chamber is induced by centrifugal rotation of the metal as a result of the interaction between the radial component of the operating current and the external magnetic flux, which is perpendicular to it. The working and electromagnet currents are generated by regulated direct current power supplies. The system controls the amount of alloy dispensed by adjusting the electromagnetic current in proportion to changes in the height of the static column (melt level), while maintaining a constant operating current. The key to regulating the amount of metal dispensed lies in controlling the two components of electromagnetic pressure necessary to elevate the molten metal to the level of the spout and to dispense it from the

spout. The necessary computations and adjustments can be handled in their entirety by analogue control devices, for example those in the UBSR-AI series. Examples of how the system would perform under different operating conditions were provided. Figures 1.

#### **Casting Finishing Operations at the Volga Automotive Plant**

917D0125C Moscow LITEYNOYE PROIZVODSTVO  
in Russian No 12, Dec 90 pp 6-8

[Abstract of article by S. I. Vasilyev, A. G. Negulyayev, and V. T. Temnikov; Volga Automotive Plant]

UDC 621.74:658.2

[Abstract] The Volga Automotive Plant's (VAZ) approach to the mechanization of foundry finishing operations, especially trimming work, entails the development and adoption of individualized trimming machines equipped with cutting tools and designed to process one casting at a time or a group of two or three related castings. Twenty-five different types of machines have been designed and built for trimming the major components of VAZ engines. These machines are simple in design, durable, reliable, easy to operate and maintain, and can handle from 200 to 500 castings per hour. They are also inexpensive, energy-efficient, quiet, and dust-free. The conveyance systems include chain conveyors for transporting large castings such as cylinder blocks, in order to take advantage of the casting shape when positioning and securing it on the conveyor, and shuttle-type conveyors with clamping devices to transport large, thin-walled aluminum castings, such as gearbox and clutch housings. Some of the machines use robots and robot arms to position the work. An example of this is a machine that is essentially a robot arm working in conjunction with a trimming press. The robot arm is used to position castings such as a cylinder heads on the loading table. The machines employ various types of electromechanical, hydraulic, and pneumatic drives to power the cutting tools. The latter include rotating tools, such as cutters, reamers, and rasps, linear-motion tools, such as mandrels, broaches, and punches, and tools that combine both types of motion. To defeat the problem of following complex contours, self-adjusting tools are used. To solve problems of tool cost, complexity, and durability, engineers are designing modular systems incorporating highly standardized machines and robots that can accommodate any number of tool fixtures. Such a system has already been built and completely mechanizes the process of trimming water pump housings.

#### **Finishing Operations at Minavtoselkhoz mash Foundries**

917D0125B Moscow LITEYNOYE PROIZVODSTVO  
in Russian No 12, Dec 90 pp 5-6

[Abstract of article by I. A. Yasevich]

UDC 621.74:658.2

[Abstract] The level of automation and mechanization in foundry finishing operations is still very low, resulting in



labor shortages and poor working conditions. Of the total labor required to produce castings, 25% is used in finishing operations, 20 to 40% of which consist of cooling and removing castings and knocking out cores, another 20 to 40% of which entail trimming, flash removal, and inspection, with the final 20% involving the removal of mold grit from castings. The Avtolitprom NPO and VNIITmash are working to develop equipment and technology to streamline these operations, with the emphasis on developing specialized versus universal equipment and modular production lines. Foundries, though, are slow to adopt new equipment and processes. In one case, 70 units of equipment produced in 1985 are not being utilized. Manufacturers of production-model trimming equipment are virtually nonexistent. A scientific and technical council made a number of recommendations for automating and streamlining foundry finishing operations. References 1: Russian.

### **Cryogenic Treatment of Castings**

917D0125A Moscow LITEYNOYE PROIZVODSTVO  
in Russian No 12, Dec 90 pp 3-4

[Abstract of article by G. M. Kimstach, B. M. Drapkin, A. A. Urtayev, Ye. C. Borisov; Rybin Institute of Aviation Technology]

UDC 621.74.002.6:621.785.92

[Abstract] Various ferrous and non-ferrous alloy castings were subjected to cryogenic treatment to determine its effect on structure and properties. White iron, grey iron, AL4 aluminum alloy, and LTs40S casting brass were made in an IST-0.16 induction furnace. The alloys were teemed into sand and clay molds. Ingots 20 mm in diameter and 110 mm in length were soaked at -196°C. The alloys were then studied metallographically on optical and electron microscopes and on a DRON-20 diffractometer and their mechanical properties tested. Cryogenic treatment substantially increased the strength and plasticity of the alloys as a result of the parallel occurrence of several processes associated with the breakdown of solid solutions. Cryogenic pre-treating can substantially accelerate the breakdown of eutectic cementite during high-temperature graphitizing of white iron, reducing the duration of this process from 30 to 50%. Cryogenic soaking also greatly improves the morphology of the eutectic cementite and the toughness of grey iron. In general, the structure and properties of all the alloys studied was improved by cryogenic treatment, which also made subsequent heat-treating processes more efficient and effective. Figures 3, tables 1.

**Brittle Failure in Steels With Developed Crystal Textures**

917D0129B Kiev AVTOMATICHESKAYA SVARKA  
in Russian No 1, Jan 91 pp 6-9

[Abstract of article by V. S. Girenko, A. V. Bernatskiy, V. M. Kozachek; Ukrainian Academy of Sciences Institute of Electric Welding imeni Ye. O. Paton]

UDC [621.791.052:669.14.018.295]:620.18:620.163.4

[Abstract] Crystallographic texture was investigated as a principle cause of brittle lamellar fractures in some types of steel. Specimens were cut from steel sheet made using controlled rolling technology. To isolate the role of crystallographic texture from the role of structural texture in this type of failure, cutting was done in the same plane in which the sheet was located, but at various angles (0, 30, 45, 60, and 90°) to the rolling direction. For further clarification, impact toughness as a function of brittle and tough fracture orientation was also measured at temperatures of 20, 0, -40, -70, -90, and -110°C. It was concluded that crystallographic texture plays a singular role in the development of brittle fractures and can predispose some types of steel to this type of failure. Figures 4; references 5: Russian.

**Improving the Induction Hard-Facing of Thin Shaped Disks**

917D0129I Kiev AVTOMATICHESKAYA SVARKA  
in Russian No 1, Jan 91 pp 57-61

[Abstract of article by Ch. V. Pulka, O. N. Shablii, Ternopol Campus of Lvov Polytechnic Institute; V. F. Grabin, I. Ya. Dzykovich, Ukrainian Academy of Sciences Institute of Electric Welding]

UDC 621.791.927.7:669.018.25:[631.33.024.3:62-415]

[Abstract] A process was developed for induction hard-facing thin disks stamped from St3 sheet steel. The process utilizes a ring inductor with a round or square winding cross-section to simultaneously surface the entire cutting edge of a disk with PG-S1 (U30Kh28N4S4) alloy. Four disks were hard-faced with the ring inductor, using different surfacing parameters for each specimen. For comparison, one disk was surfaced using a conventional process, which employs a segmented inductor. The dimensions, structure, and microhardness of the hard facing on all of the specimens were of comparable quality, but two of the induction-surfaced disks were more wear-resistant. These disks underwent a two-stage heating process that made it possible to control the layer-by-layer redistribution of chromium and carbon throughout the thickness of the deposited metal, thereby increasing their content in the surface layers and resulting in the formation of (Fe,Cr)<sub>7</sub>C<sub>3</sub> carbides. Another major advantage of the new process is that heating is more uniform, and, as a result, the thickness of the deposited metal is more

uniform and there is less deformation of the disk. The new process is also 4 to 5 times more productive than the conventional process. Figures 7, tables 2; references 5: Russian.

**Capacitor-Discharge Welding and Mechanical Properties of Aluminum Alloy Fasteners**

917D0129H Kiev AVTOMATICHESKAYA SVARKA  
in Russian No 1, Jan 91 pp 53-56

[Abstract of article by D. M. Kalenko, N. A. Chvertko, Ukrainian Academy of Sciences Institute of Electric Welding; G. P. Tsarkov, S. A. Gusakov, Scientific Production Association imeni S. A. Lavochkina, Moscow]

UDC [621.791.75:621.319.4].002:669.715.62-23

[Abstract] A special welding gun, model N148, was developed for welding aluminum alloy fasteners such as rivets and studs to aluminum sheet. The gun utilizes a capacitor-discharge percussion process to weld the fasteners to the sheet. A special chock, part no. N148.05.000, was also developed to hold fasteners in the gun during the welding process. Essentially, the gun works by simultaneously firing a fastener against the sheet to which it is to be welded and supplying capacitor voltage to the work. The fasteners used in this type of welding gun are made with stems that have a single nib 1.5 mm in diameter and length. As the fastener is fired, its nib makes contact with the sheet and explodes, the capacitor arc is struck, and the surfaces are fused, welding the fastener to the surface of the sheet. The gun was tested using button rivets made from AMg3M aluminum alloy, studs made from AMg6M aluminum alloy, and AMg6M aluminum alloy sheet 1.5, 2.0, and 3.0 mm thick. Optimal welding parameters were: capacitance - 70 mF; capacitor voltage - 140 V; initial compressive force of tensioning spring - 92 N; and size of gap between work and fastener—3 mm. These parameters were employed to assemble weldments simulating actual assemblies, which were subjected to a variety of tests for strength, durability, and resistance to various types of mechanical stress. The quality of the welds was high, and the welded assemblies were able to withstand severe tearing, twisting, and bending and repeated assembly and disassembly while maintaining functional characteristics. The new technique reduces electricity consumption 10-fold, eliminates the need for costly materials, reduces the weight of the welded assemblies, and increases labor productivity and working conditions. Figures 5, tables 1, references 2: Russian.

**Using an Electromagnetic Sprayer to Apply Coatings**

917D0129J Kiev AVTOMATICHESKAYA SVARKA  
in Russian No 1, Jan 91 pp 66-68

[Abstract of article by A. I. Ponomarev, B. V. Danilchenko, G. A. Kirilyuk; Ukrainian Academy of Sciences Institute of Electric Welding imeni Ye. O. Paton]

UDC 621.793.03.002.237:538.3

[Abstract] The use of an electromagnetic sprayer to propel thermally sprayed coatings was investigated. An electromagnetic sprayer works on the principle of an electromagnetic catapult. A discharge is created between two parallel electrodes connected to a power supply. The discharge plasma is accelerated by electromagnetic forces and propels the spray particles at speeds of up to 10 to 20 km/second. An experimental electromagnetic sprayer was tested. It consisted of two copper electrodes 50 mm long connected to a d.c. power supply to create a 50-kA circuit. Sv-08A wire was fed into the gap between the electrodes, where the end of the wire was atomized, and the particles propelled vertically for a distance of 6 to 10 m. Although this experiment demonstrated that electromagnetic sprayers are feasible, their commercial usefulness is hampered by the relatively large amounts of current they require. To make the devices more energy efficient, experimental electromagnetic sprayers have been developed that utilize an external magnetic field source to help propel the spray particles. They consist of the electrodes, which can either be nonconsumable or consumable in the form of the feed wire, an electromagnetic winding, and either an electromagnetic core or a magnetic conductor. The wire is atomized and propelled by the force of the current flowing through it in a direction perpendicular to the induction vector of the magnetic field source. In the case of the consumable electrodes, they serve as the "rails" between the magnetic poles. The permanent electrode sprayer was used to spray Sv-15GSTYuTsA wire onto a plate of St3 steel. The coating had a homogenous structure, less than 4% porosity, and a small quantity of oxide interlayers between grains. Thus, electromagnetic sprayers can produce coatings superior to those applied by conventional means, partially justifying their high energy consumption. Figures 5; references 8: Russian.

#### Temperature Field and Phase Composition of Metal in the Heat-Affected Zone During Underwater Welding

917D0129F Kiev AVTOMATICHESKAYA SVARKA in Russian No 1, Jan 91 pp 45-47

[Abstract of article by S. F. Budz, B. D. Drobenko, V. I. Astashkin, T. N. Ivanchova of the All-Union Central Institute of Applied Mechanics and Mathematics of the Ukrainian Academy of Sciences, Lvov; I. M. Savich, A. L. Kuporev of the Ukrainian Academy of Sciences Institute of Electric Welding imeni Ye. O. Paton]

UDC 621.791.755:536.42.517.549.8

[Abstract] The phase composition of metal in the heat-affected zone (HAZ) of a 10-mm plate of 17G1S steel pipe and the temperature field of the specimen during underwater welding were studied to learn more about how underwater welding conditions affect weld quality. The temperature field was measured using a model that takes into account the presence of liquid, solid, and

transition states in the metal as well as the radiative and convective heat transfer occurring between the heated surface of the plate and the water. The model assumes that change in the phase composition of the liquid-to-solid transition region does not depend on the heating and cooling rates and is described by a linear function of temperature. The finite element method was used in conjunction with the -method family to perform the calculations in FORTRAN. Because of the rapid rate at which the metal is cooled underwater, quenched martensite and bainite are formed, resulting in the appearance of residual stresses, embrittlement of the metal, and deterioration in weldment strength. The theoretical calculations yielded a relationship between martensite content in the metal of the HAZ and welding speed. Minimum martensite content was achieved when welding speed was 2 mm/second, as the lower speed resulted in a higher heating temperature and a slower cooling rate for the metal. Figures 3; references 6: Russian.

#### Effect of Load Frequency on Steel and Weld Fatigue Resistance

917D0129E Kiev AVTOMATICHESKAYA SVARKA in Russian No 1, Jan 91 pp 30-34

[Abstract of article by V. S. Kovalchuk, Ukrainian Academy of Sciences Institute of Electric Welding]

UDC [621.791.052:669.18]:620.178.311.82.001.24

[Abstract] The effect of infrasonic frequencies on the fatigue resistance of base and welded engineering steels was studied. Specimens made from M16S, 22K, and high-strength steels with artificial stress concentrators, MSt3kp steel lap welds made with UONI-13/45 electrodes, and 20K steel butt welds made with a semiautomatic welder using Sv09 wire and An-348 flux were subjected to axial tensile testing starting with a tensile load of zero. Load frequencies were 5 to 800 cycles/minute for the base steels, 20 to 30 and 300 cycles/minute for the lap welds, and 3 and 300 cycles/minute for the butt welds. For all the specimens, testing was ceased during the initial stages of fatigue crack development, when the cracks were 2 to 3 mm deep. The results showed that reducing the load frequency from a range of 800 to 300 to a range of 30 to 3 cycles per minute had no effect on the fatigue resistance of high-strength steel specimens, but reduced the life of the low-carbon and austenitic steel specimens 1.5 to 3-fold. The latter effect was intensified at higher levels of stress concentration. The largest drop in fatigue resistance occurs within the 200 to 30 cycles per minute range and reaches 20 to 40 MPa depending on the steel and the level of stress concentration. Figures 3; references 13: 11 Russian, 2 Western.

**Controlling Metal Transfer With Pulsed MIG Welding**

917D0129G Kiev AVTOMATICHESKAYA SVARKA  
in Russian No 1, Jan 91 pp 48-52

[Abstract of article by V. Senchak, P. Orsag; Welding Research Institute, Bratislava, Czechoslovakia]

UDC 621.791.754'29)5:621.3.014.33

[Abstract] Metal transfer and welding process stability during pulsed MIG welding was studied. The research was carried out on a VUZ-L3 welder controlled by an SM 4-20 computer. A Union Carbide MIGPULSE 402 transistor-type power supply provided direct current to a reverse polarity welding set-up. The base metal was a plate of ChSN 11373 low carbon steel on which a weld bead was deposited. A consumable electrode of C 123 wire 1.2 mm in diameter was fed into the arc at a rate of 1.6 to 25.1 meters per minute. The shielding gas, which was consumed at a rate of 10 to 15 liters per minute, was 90% argon and 10% carbon dioxide. Base current ranged from 5 to 406 A, base (pause) duration from 1 to 20.1 ms, pulse voltage from 0.4 to 41.4 V, and pulse duration from 1.1 to 10.2 ms. The results of varying the different welding parameters indicated that welding parameter values that will ensure a stable welding process are dependent on the electrode feed rate. Thus, when increasing the feed rate, the base duration should be decreased; in other words, pulse frequency should be increased. The reverse is also true. A stable welding process was achieved when pulse voltage was 36 V, base current was 50 A, the wire feed rate was 2.8 to 10.0 meters per minute, pulse duration was 2.2 ms, and base duration was 0.9 to 20.0 ms (experimental minimum to maximum values), depending on the wire feed rate. Theoretical calculations yielded a base duration range of 1.2 to 25.6 ms. This data was used to set up a one-touch method of controlling pulsed MIG welding parameters, wherein the MIGPULSE 403 was connected to a computer that adjusted pulse values according to the electrode wire feed rate. Figures 4, tables 1; references 10: 1 Russian, 2 East European, 7 Western.

**Estimating the Effect of Residual Stresses on Low-Cycle Weld Fatigue**

917D0129C Kiev AVTOMATICHESKAYA SVARKA  
in Russian No 1, Jan 91 pp 17-22

[Abstract of article by V. I. Makhnenko, R. Yr. Mosenkis; Ukrainian Academy of Sciences Institute of Electric Welding imeni Ye. O. Paton]

UDC [621.791.052:669.15-194.2]:539.4.014:539.43

[Abstract] Theoretical modules were developed that will enable engineers to use an existing computer program to take the effects of residual stresses into account when

calculating low-cycle weld service life. Satisfactory agreement was obtained between the theoretical and experimental data on residual stresses arising longitudinally and transversely in relation to the external load. The theoretical constructs were used to calculate the effects of residual welding stresses, including relaxation, on low-cycle weld service life. It was found that, the smaller the load and/or the stronger the base metal, the greater the effect of residual stresses. The unrelaxed component of residual stresses is critically important to low-cycle weld service life. If the direction of residual stresses coincides with the load direction, then their effect can be measured by using a new value for load cycle asymmetry. The extent to which residual tensile stresses in a weld bearing a shearing load affect its service life also depend on the extent to which these stresses are relaxed. Since residual tensile stresses relax much quickly than residual shear stresses in a weld subjected to a tensile load, their effect on low-cycle fatigue is much less noticeable. Figures 6; references 8: 7 Russian, 1 Western.

**Holographic Measurement of Residual Stresses in Butt-Welded 12Kh2N4MD Steel**

917D0129D Kiev AVTOMATICHESKAYA SVARKA  
in Russian No 1, Jan 91 pp 26-29

[Abstract of article by L. M. Lobanov, V. A. Pivtorak, G. V. Cherkashin, Ukrainian Academy of Sciences Institute of Electric Welding imeni Ye. O. Paton; T. G. Shubladze, G. S. Vachiberadze, Kutais Polytechnic Institute]

UDC

[621.791.72.052:669.14.018.295]:539.4.014:778.38

[Abstract] A study was done to determine the relationship between the accuracy of residual stress measurements and the amount of cold work that takes place when drilling holes for the purpose of measuring residual stresses in welded joints (Matar test). A highly accurate (approximately 1  $\mu$ m) portable holograph was used to record surface point displacement in the area of the hole without making contact with the specimen. Three specimens of pre-heat-treated welded 12Kh2N4MD steel 57 mm thick were used in the study. A series of double-exposure holographs was taken for each specimen. Between exposures, holes 1, 1.5, 2, 2.5, and 3 mm in diameter were drilled in the specimens. In each case, hole depth was equal to hole diameter. R6M5 drill bits with a 120° point angle were used to drill the holes. The first series of holes of a particular diameter was drilled using a fresh bit. The last series of holes of a particular diameter was drilled after the bit had been used to drill 50 holes without being resharpened. Examination of the specimens revealed that, the larger the bit, the more worn it was, and the harder the metal, the greater the extent of plastic deformation in the metal around the hole. This information was used successfully to calculate measurement error as a function of drill bit size and

metal hardness and to determine how often drill bits should be sharpened. These relationships can be used to estimate residual stresses in welds and weldments. Figures 7; references 3: Russian.

**Stress Distribution Along Fillet-Welded T-Joints  
Between Elements of Limited Rigidity**

917D0129A Kiev AVTOMATICHESKAYA SVARKA  
in Russian No 1, Jan 91 pp 1-6

[Abstract of article by V. I. Makhnenko, Ye. A. Velikoi-  
vanenko, G. F. Rozyuka; Ukrainian Academy of Sci-  
ences Institute of Electric Welding imeni Ye. O. Paton]

UDC [621.791.052:669.15-194]:539.4.001.24

[Abstract] A theoretical algorithm was constructed for the purpose of estimating the degree of non-uniform stress distribution along the length of fillet-welded T-joints depending on joint geometry, cross-section size, and the properties of the weld metal. The algorithm was also used to obtain data on the ultimate load for a particular weld. The results of calculations performed using the algorithm were presented and were found to be highly consistent with the results of experimental studies. Both sets of data indicate that stress distribution along fillet-welded T-joints between elements of limited rigidity in a weldment subjected to typical external stresses can substantially differ from uniform values. Figures 6, tables 3; references 5: 3 Russian, 2 Western.

**A Hydrodynamic Theory of Mass Transfer Anomaly in Solid Bodies Subjected to Shock**

917D0130F Kiev METALLOFIZIKA in Russian No 1, Jan 91 pp 124-127

[Abstract of article by B. V. Yegorov, L. O. Zvorykin, B. B. Timofeyev; Institute of Physical Metallurgy of the Ukrainian Academy of Sciences]

UDC 539.219.3:53.09

[Abstract] A theory of mass transfer anomaly was constructed using hydrodynamic equations to describe the irreversible phenomena occurring in the front of the shock wave and associated with an increase in the entropy of the system. This increase in entropy is determined solely by the beginning and ending states of the body and should result from the dissipation processes occurring in the wave front itself. The dissipation processes, in turn, are associated with thermal conductivity and viscosity, the latter being a characteristic not only of the medium, but also a function of the pressure gradient and the specific volumes in front of and behind the front of the shock wave. References 5: Russian.

**Linear Creep Limit in One- and Two-Dimensional Aluminum Polycrystals**

917D0130D Kiev METALLOFIZIKA in Russian No 1, Jan 91 pp 116-120

[Abstract of article by Ye. Ye. Badiyan, V. B. Rabukhin, A. G. Tonkopryad; Kharkov State University]

UDC 669.71:539

[Abstract] Creep behavior was studied in aluminum specimens with parqueted (two-dimensional) and "bamboo" (one-dimensional) structures, with the latter made from the former by cutting shavings with a width not exceeding the average grain size of 1.5 to 20 mm from along the length of the specimens. Tests were performed at 100°C within a wide range of creep-inducing stresses. All of the creep vs stress curves were similar for all specimen pairs and typically had a linear and a non-linear part, with the transition between the two occurring quite abruptly as stress was increased. The stress corresponding to this transition is the linear creep limit, and it was always lower in the two-dimensional specimens, which had triple-jointed borders, than in the one-dimensional ones. As grain size decreased (triple joint density increased), the difference in the values for the linear creep limit increased. It is likely that the inclusion of dislocations during the process of diffusion creep induces a threshold point in polycrystals, as it does in monocrystals. Figures 2; references 9: 8 Russian, 1 Western.

**Thermal Conductivity of Berillium as a Function of Temperature Between 15 and 275 K**

917D0130D Kiev METALLOFIZIKA in Russian No 1, Jan 91 pp 112-116

[Abstract of article by S. A. Guzhva, F. F. Lavrentyev, P. K. Kolesnikov, O. V. Matsiyevskiy; Institute of Applied Low-Temperature Physics of the Ukrainian Academy of Sciences, Kharkov]

UDC 536.21

[Abstract] The coefficient of thermal conductivity ( $\lambda$ ) as a function of temperature was studied in three types of commercial-grade berillium. Be<sub>I</sub> was produced by hot pressing, Be<sub>II</sub> by forging, and Be<sub>III</sub> by isostatic pressing. Impurity percentages were 2.2%, 1.3%, and 1%, respectively. Specimens were cut from the billets along and against their axes to form 5 x 5 bars about 100 mm in length and then heat treated. An experimental device working on the same principle as a thermal potentiometer was used to statically measure  $\lambda$ . The  $\lambda(T)$  curves were the same for all three materials and typical for materials with high concentrations of impurities. Up to about 90-100 K, the relationship was linear, with the maximum reached between 150 and 180 K. On the linear sections of the curves, the value for  $\lambda$  was virtually identical for all specimens. It was concluded that the electron component is the most important determinant of thermal conductivity at temperatures up to and including 220 K. At higher temperatures, the background component becomes substantial. Electron scattering on the impurities predominates when the relationship is linear. Above 100 K, electron scattering on the background is more predominant, and the linear relationship is disrupted, causing noticeable anisotropy in  $\lambda$  for B<sub>I</sub>. The degree of electron-background interaction varies according to the direction in which a specimen was cut from the billet. For all temperatures and specimens,  $\lambda$  was slightly higher for lengthwise-cut specimens. The degree of anisotropy for the forged specimens was much lower than for the hot-pressed specimens, while the isostatically pressed specimens were virtually isotropic throughout the temperature range studied. Figures 1, tables 2; references 6: 2 Western, 4 Russian.

**Certain Features of  $\gamma$ -Fe Crystal Formation in Fast-Quenched Fe<sub>85</sub>B<sub>15</sub> Alloy**

917D0130C Kiev METALLOFIZIKA in Russian No 1, Jan 91 pp 77-83

[Abstract of article by A. P. Brovko, L. Ye. Mikhaylova, and A. V. Romanova; Institute of Physical Metallurgy of the Ukrainian Academy of Sciences, Kiev]

UDC 539.26:539.216

[Abstract] The structure of fast-quenched Fe<sub>85</sub>B<sub>15</sub> alloys containing  $\gamma$ -Fe microcrystalline particles was studied in

greater detail than in previous studies. Tests were performed on a DRON-3 with a graphite monochromator and on an apparatus of original design consisting of a coordinate detector and a multi-channel analyzer. The x-ray diffraction patterns were used to calculate  $i(s)$  structural factors and functions for the radial distribution of atoms and to evaluate the structural state of the surface layers of alloy strip. Two types of tests were performed on the other apparatus. One involved measuring the intensity of small-angle x-ray distribution "during transmission" to determine crystalline particle size from 1-15 nm. The other test utilized the "reflection" to directly observe quickly occurring changes in the region of first diffraction maximum during isothermal annealing. During annealing at 560°C, a  $\gamma$ -Fe to  $\alpha$ -Fe transformation occurs over a lengthy period of time, indicating that the  $\gamma$ -Fe crystals on the contact surface are metastable. During x-ray diffraction testing, strip specimens were placed in three different positions relative to the goniometer's rotational axis—parallel, antiparallel, and perpendicular. The structural factor and radial distribution results showed that this alloy would conventionally be classified as x-ray amorphous, although the height of the first maximum is somewhat greater than usual for this type of alloy. Also, the first maximum height was greater for all specimens when they were in the parallel position. The other characteristics remained unchanged regardless of specimen position. The x-ray diffraction tests also revealed that the  $\gamma$ -Fe microcrystalline particles formed in the contact surface of strip quenched from 1390°C are textured, with the degree of texture increasing the greater the distance from the beginning of the strip. Figures 4; references 7: Russian.

#### Monitoring of Operation of the Drives of Pulsating-Bottom Furnaces

917D0115G Moscow METALLOVEDENIYE I  
TERMICHESKAYA OBRABOTKA METALLOV  
in Russian No 12, Dec 90 pp 40-41

[Article by T.A. Vorobyeva and L.F. Liberman, OVNI-IETO (not further identified), Istra]

UDC 621.783.23

[Abstract] Variations in the operation of cam-type or hydraulic pulsation-inducing mechanisms for reheating-furnace bottom plates result in changes in the speed of travel of the articles being reheated and consequently in unpredictable changes in reheating time. A direct observation of these changes is impossible. A system is described that measures and records the forward travel of an inert body sliding on guides installed on the wall of the bottom-plate table on which the articles being reheated travel within the furnace. The sliding body simulates the travel of the articles. It is connected to the arm of a rheostat, and the change in the rheostat voltage is proportional to the distance the sliding body travels during one forward-and-backward cycle of the bottom

plate. A change in the distance traveled by the sliding body during one cycle indicates that the pulsation mechanism requires adjustment or maintenance. Figures 2; one Russian reference.

#### A One-Dimensional Model of Thin-Film Growth

917D0130B Kiev METALLOFIZIKA in Russian No 1,  
Jan 91 pp 59-67

[Abstract of article by A. V. Osipov, Leningrad Branch of the Institute of Machine Science, USSR Academy of Sciences]

UDC 539.216.2

[Abstract] A model was formulated to describe the process by which a substrate is filled in by clusters until a solid film is formed. The model is relatively simple, yet describes a number of phenomena and dispenses with the distinction between solid-phase sintering and liquid-coalescence. The model posits an infinite straight line on which one-dimensional nuclei can form. Their length is proportional to the number of particles they contain. When two clusters merge, the new cluster has the same shape and has the length of the two original clusters. A function for cluster distribution by size is introduced and normed to yield a number of clusters per unit of substrate length. This distribution should conform to the kinematic coagulation equation. The coagulation center model is simplified so that it is dependent only on time. New dimensionless variables are introduced, and the coagulation equation incorporating the simplified model for the coagulation center is solved to obtain the equation representing nuclei coalescence in thin films. This equation is then used as the basis for calculating the function for cluster distribution by size, its enumerable moments, the extent to which a substrate is filled in by clusters and cluster concentration for some of the most important special cases. The results obtained are qualitatively compatible with those obtained from the Kolmogorov model and from numerical modeling. References 18: 6 Western, 12 Russian.

#### Magnetoelastic Effects in Weakly Ferromagnetic Alloys

917D0130A Kiev METALLOFIZIKA in Russian No 1,  
Jan 9 pp 32-37

[Abstract of article by A. A. Povzner and A. G. Volkov, Ural Polytechnic Institute, Sverdlovsk]

UDC 538.95.951

[Abstract] Spin density concentration fluctuations, which cause magnetization isotherms to deviate from the Belov-Arrat laws, were studied to determine their influence on magnetically induced thermal expansion and the bulk compression modulus. The thermodynamic

potential of the d-electron system of a weakly ferromagnetic alloy was calculated, allowing for electron movement within the lattice crystalline potential field and for electron-electron interaction at the nodes, which are occupied by atoms of the transition metal. The calculations used result in an expression for thermodynamic potential in the form of functional integrals. This expression was further modified to obtain an expression for the magnetic part of thermodynamic potential. The results of these calculations were used to analyze the effect of magnetism on thermal expansion and the compression modulus. The results showed that both spin density concentration fluctuations and thermodynamic spin fluctuations determine the extent to which magnetism both positively and negatively affects thermal expansion and the extent to which compression moduli are affected by temperature in these alloys. Figures 1, tables 1; references 10: 6 Western, 4 Russian.

#### **New Refractory Compositions for Closing of Iron Notches and Ramming of Runners**

917D0120C Moscow METALLURG in Russian No 12, Dec 90 p 36

[Article by V.M. Gorobtsov, V.N. Belyakov, V.F. Sereda, N.T. Danayev, A.M. Pecherkin, V.I. Derkach, and G.M. Nikitin, Karaganda Metallurgical Combine and Chemistry and Metallurgy Institute of the Kazakh SSR Academy of Sciences]

[Abstract] A cheaper refractory composition for closing of iron notches at the Karaganda Metallurgical Combine blast-furnace shop was produced by substituting moist molding sand (1.4 rubles/ton) for part of crushed coke (35 rubles/ton), fireclay powder (20 rubles/ton), and clay without impairing the quality of the composition. In addition to reduced cost, the new composition creates less dust at the composition preparation location. The new composition contains 32 percent coke, 10 percent clay, 30 percent molding sand, 4 percent pitch, and 24 percent coal tar. The old composition contained 34-36 percent crushed coke 20-24 percent fireclay powder, 12-16 percent ground refractory clay, 4-5 percent pitch, and 23-25 percent coal tar. The runner lining life was increased from 7 to 10 days in the case of blast furnaces with 2 iron notches and from 14 to 20 days in the case of blast furnaces with 3 and 4 iron notches by changing the ramming mix composition from 15-17 percent coal pitch, 65-68 percent crushed coke, and 18-20 percent ground refractory clay to 18 percent pitch, 66 percent coke, and 16 percent clay and by changing the initial heat treatment from heating at a rate of 500-600°C to drying

for 1 h at 100-110 °C, heating for 20 minutes at 350-400°C, and heating at a rate of 600-700°C in order to slow down the escape of volatiles and prevent cracking of the lining.

#### **The Future of Sheet and Plate Production**

917D0120A Moscow METALLURG in Russian No 12, Dec 90 pp 34-35

[Article by D. Zheleznov, Moscow Steel and Alloy Institute]

[Abstract] Improvement of properties of carbon and low-alloy steels by optimization of rolling and heat-treatment practices in order to produce custom steels with guaranteed properties is proposed as an economical alternative to expensive high-alloy steels for articles and structures in which lightweight design is of paramount importance. Theoretical and experimental data regarding the structure and texture transformations as a function of alloy production practice, mechanical working, and heat treatment are already available as a result of research in the Soviet Union and can be used in the development of thermomechanical, laser, and chemical treatment practices required to produce steels with high, guaranteed properties. Custom-designed steels are particularly attractive for mass-production applications, such as transportation equipment and domed buildings, where the steel production volume justifies the expense of development of custom steels. Development of custom steels requires close collaboration between the steel producers and users.

#### **Will Fines Protect the Environment?**

917D0120A Moscow METALLURG in Russian No 12, Dec 90 pp 27-29

[Article by I. Dnepryanko and A. Simagov, Zaporozhye, Donetsk, Moscow]

[Abstract] Problems with pollution abatement in Zaporozhye and vicinity are discussed. In Zaporozhye there are 1089 industrial sources of air pollution and 110 sources of water pollution that lack pollution controls. Funds allocated for pollution control equipment are frequently not spent because there is a severe shortage of pollution control manufacturing facilities. Also, building contractors receive special incentives for building manufacturing facilities but not for building pollution control equipment. Fines imposed on industrial polluters by local authorities are frequently misspent on beautification equipment, such as power mowers and special brooms, depriving the manufacturing enterprises of funds that could be used for fighting pollution. Only a joint effort by enterprises, ecology organizations, scientists, and authorities can alleviate the pollution problems; fines should merely serve as stimuli for action.



NTIS  
ATTN: PROCESS 103

2

5285 PORT ROYAL RD  
SPRINGFIELD, VA

22161

This is a U.S. Government publication. Its contents in no way represent the policies, views, or attitudes of the U.S. Government. Users of this publication may cite FBIS or JPRS provided they do so in a manner clearly identifying them as the secondary source.

Foreign Broadcast Information Service (FBIS) and Joint Publications Research Service (JPRS) publications contain political, military, economic, environmental, and sociological news, commentary, and other information, as well as scientific and technical data and reports. All information has been obtained from foreign radio and television broadcasts, news agency transmissions, newspapers, books, and periodicals. Items generally are processed from the first or best available sources. It should not be inferred that they have been disseminated only in the medium, in the language, or to the area indicated. Items from foreign language sources are translated; those from English-language sources are transcribed. Except for excluding certain diacritics, FBIS renders personal and place-names in accordance with the romanization systems approved for U.S. Government publications by the U.S. Board of Geographic Names.

Headlines, editorial reports, and material enclosed in brackets [ ] are supplied by FBIS/JPRS. Processing indicators such as [Text] or [Excerpts] in the first line of each item indicate how the information was processed from the original. Unfamiliar names rendered phonetically are enclosed in parentheses. Words or names preceded by a question mark and enclosed in parentheses were not clear from the original source but have been supplied as appropriate to the context. Other unattributed parenthetical notes within the body of an item originate with the source. Times within items are as given by the source. Passages in boldface or italics are as published.

#### SUBSCRIPTION/PROCUREMENT INFORMATION

The FBIS DAILY REPORT contains current news and information and is published Monday through Friday in eight volumes: China, East Europe, Soviet Union, East Asia, Near East & South Asia, Sub-Saharan Africa, Latin America, and West Europe. Supplements to the DAILY REPORTs may also be available periodically and will be distributed to regular DAILY REPORT subscribers. JPRS publications, which include approximately 50 regional, worldwide, and topical reports, generally contain less time-sensitive information and are published periodically.

Current DAILY REPORTs and JPRS publications are listed in *Government Reports Announcements* issued semimonthly by the National Technical Information Service (NTIS), 5285 Port Royal Road, Springfield, Virginia 22161 and the *Monthly Catalog of U.S. Government Publications* issued by the Superintendent of Documents, U.S. Government Printing Office, Washington, D.C. 20402.

The public may subscribe to either hardcover or microfiche versions of the DAILY REPORTs and JPRS publications through NTIS at the above address or by calling (703) 487-4630. Subscription rates will be

provided by NTIS upon request. Subscriptions are available outside the United States from NTIS or appointed foreign dealers. New subscribers should expect a 30-day delay in receipt of the first issue.

U.S. Government offices may obtain subscriptions to the DAILY REPORTs or JPRS publications (hardcover or microfiche) at no charge through their sponsoring organizations. For additional information or assistance, call FBIS, (202) 338-6735, or write to P.O. Box 2604, Washington, D.C. 20013. Department of Defense consumers are required to submit requests through appropriate command validation channels to DIA, RTS-2C, Washington, D.C. 20301. (Telephone: (202) 373-3771, Autovon: 243-3771.)

Back issues or single copies of the DAILY REPORTs and JPRS publications are not available. Both the DAILY REPORTs and the JPRS publications are on file for public reference at the Library of Congress and at many Federal Depository Libraries. Reference copies may also be seen at many public and university libraries throughout the United States.